6.01 III-Nitride-Based Short-Wavelength Ultraviolet Light Sources

A Khan and K Balakrishnan, University of South Carolina, Columbia, SC, USA

Glossary

Aluminum gallium nitride ($Al_xGa_{1-x}N$) A wide-band-gap semiconductor material with very nearly the same lattice constant as GaN but a larger band gap. The lattice constant (or lattice parameter) refers to the constant distance between unit cells in a crystal lattice. Lattices in three dimensions, generally, have three lattice constants, referred to as *a*, *b*, and *c*. The *x* in the formula is a number between 0 and 1. This indicates an arbitrary alloy between GaN and aluminum arsenide, AlAs, which is a semiconductor material with almost the same lattice constant as gallium arsenide and aluminum gallium arsenide and wider band gap than GaAs . . . AlN The band gap varies between 3.4 (GaN) and 6.2 eV (AlN). AlGaN should be considered as an abbreviated form of the above, rather than any particular ratio. AlGaN is used to manufacture light-emitting diodes operating in blue to deep ultraviolet (DUV) region, where wavelengths down to 210 nm have been achieved. It is also used in blue and UV semiconductor lasers, detectors of UV radiation, and in AlGaN/GaN high-electron-mobility transistors.

Aluminum nitride (AlN) A nitride of aluminum. Its wurtzite structural phase is an extremely wide-band-gap (6.2 eV) semiconductor material which has major application in DUV optoelectronics.

Deep ultraviolet (DUV) This refers to UV-B (290–320 nm) and UV-C (200–290 nm) regions of electromagnetic spectrum.

Gallium nitride (GaN) The most prominent group-III-nitride semiconductor with a direct band gap of 3.4 eV. It crystallizes in hexagonal wurtzite and cubic zincblende structural phases. It is predominantly used in optoelectronic, high-power, and high-frequency devices.

Hydride-vapor-phase epitaxy (HVPE) An epitaxy process that is used for depositing compound semiconductors. As an epitaxy technique that works near the thermodynamic equilibrium, it is of particular interest for applications such as selective area growth, planar growth. and overgrowth of buried structures. This process offers the opportunity to efficiently manufacture extremely thick and pure compound semiconductor structures, such as substrates or templates of GaN, and AlN.

Indium gallium nitride ($In_xGa_{1-x}N$) A type of semiconductor material used in manufacturing blue LEDs and other electronic devices. The *x* in the formula is a number between 0 and 1. This indicates an arbitrary alloy between InN and aluminum arsenide, AlAs, which is a semiconductor material with almost the same

lattice constant as gallium arsenide and aluminum gallium arsenide and wider band gap than GaAs . . . GaN. The band gap varies between 0.6 eV (GaN) and 3.4 eV (AlN). Active regions in most of the III-nitride-based green and blue LEDs and LDs are composed of InGaN.

LD (LD) A semiconductor device that emits coherent light when forward biased.

Light-emitting diode (LED) A semiconductor LED is a solid-state device that emits incoherent light in a narrow spectral range when forward biased. An LED consists of a p–n junction with a multiple quantum-well (MQW) active region and carrier confining layers. The p-region contains positive electrical charges, while the n-region contains negative electrical charges. When voltage is applied and current begins to flow, the electrons move across the n-region into the p-region. The process of an electron moving through the p–n junction releases energy. The dispersion of this energy produces photons with visible, infrared, and UV wavelengths depending on the energy gap (Eg) of the material used in the active region of the LED. The performance of an LED is characterized by its wall-plug efficiency, which is the optical power output of the LED divided by the electrical power supplied to the device. This is a function of internal quantum efficiency (number of photons generated in the active region per electrons injected into the LED) and extraction efficiency (number of photons that are emitted from the LED chip per photons generated in the active region). External quantum efficiency (EQE) is the product of the internal quantum efficiency and extraction efficiency.

Migration-enhanced metal-organic chemical-vapor deposition (MEMOCVD) In MEMOCVD, the duration of group III and group V pre-cursor pulses is further optimized in a pattern that allows a beneficial surface migration of reacting species on the growing film. This allows to change the V/III ratio from almost zero to several thousands, which greatly increases the probability that the Al and Ga adatoms migrate to their appropriate sites in the lattice. High quality AlN and AlN/AlGaN superlattices are reported to be grown by this method. AlGaN device structures deposited over MEMOCVD grown AlN and AlN/AlGaN superlattices are also determined to be of superior quality, in terms of structure and minority carrier lifetime. These MEMOCVD buffers are used for the fabrication of high-power deep-UV LEDs.

Metal-organic chemical-vapor deposition (MOCVD) A method to deposit semiconductor materials by allowing gaseous sources to react on the surface of a semiconductor and form another perfect crystal semiconductor on the surface. With this compound semiconductor production method, the raw material metallo-organic compounds are transformed into gases and, then, bound to a carrier gas, are fed into the reactor. This transformation also occurs under reduced pressure, around one-tenth of normal atmospheric pressure. MOCVD equipment allows the processing of quite large surface areas and is therefore first choice for the production of compound semiconductors.

MOHVPE A combination of MOCVD and HVPE epitaxy techniques carried out using a single chamber often to deposit thick semiconductor templates followed by device structures.

n-Type semiconductor A semiconductor that is doped with an electron donor is called 'n-type material'. In the case of III-nitride semiconductors, silicon (Si) is predominantly used as the n-type dopant.

Optical pumping The excitation of the lasing medium by the application of light rather than electrical discharge.

Optically pumped lasers A type of laser that derives energy from another light source, such as a xenon or krypton flash lamp or other laser source.

Quantum efficiency (QE) In an optical source or detector, the ratio of the number of generated photons per second to the number of electrons flowing per second.

Pulsed atomic layer epitaxy (PALE) A special modification of the MOCVD technique for depositing III-nitride thin films and related device structures. The unique feature of PALE is the self-limiting film growth mechanism which gives it a number of attractive properties, such as accurate and simple film thickness control, sharp interfaces, uniformity over large areas, good reproducibility, multilayer processing capability, and high film qualities at relatively low temperatures. By employing this technique, a drastic reduction of parasitic reactions between group III and nitrogen species can be achieved.

p-Type semiconductor A semiconductor that is doped with an electron acceptor is called the p-type semiconductor. In the case of III-nitride semiconductor devices, magnesium (Mg) is predominantly used as the p-type dopant.

Quantum-confined Stark effect (QSCE) This describes the effect of an external electric field upon the light absorption spectrum of a quantum-well (QW). In the absence of an external electric field, electrons and holes within the QW may only occupy states within a discrete set of energy subbands. As a consequence, only a discrete set of frequencies of light may be absorbed by the system. When an external electric field is applied, the electron states shift to lower energies, while the hole states shift to higher energies. This reduces the permitted light-absorption frequencies. In addition, the external electric field shifts electrons and holes to opposite sides of the well, reducing the absorption coefficient of the system. The spatial separation between the electrons and holes is limited by the presence of the potential barriers around the QW, indicating that excitons are able to exist in the system even under the influence of an electric field. QSCE is commonly observed in wurtzite III-nitride device structures.

Semiconductor laser In a semiconductor laser or laser diode, the active medium is a semiconductor similar to that found in an LED. The most common and practical type of laser diode is formed from a p–n junction and powered by injected electric current. These devices are sometimes referred to as 'injection laser diodes'.

Thermal management of UV LEDs The methods adopted to lower the junction temperature in a UV LED in order to achieve optimum performance. If thermal management is not considered, the LED will fail or its lifetime will be significantly decreased.

UV radiation The electromagnetic radiation with wavelengths between soft X-rays and visible violet light, often broken down into UV-A (320–400nm), UV-B (290–320 nm), UV-C (200–290 nm), and vacuum UV (10–200 nm). UV radiation of wavelengths less than 180 nm is transmitted very poorly through air.

Visible radiation Often referred to as light, this is the electromagnetic radiation which can be detected by the human eye. It is commonly used to describe wavelengths which lie in the range between 380 and 780 nm.

6.01.1 Introduction

Group-III-nitride-based short-wavelength ultraviolet (UV) light sources, such as laser diodes (LDs) and light-emitting diodes (LEDs), with active region comprising AlInGaN material system that can emit light at a wavelength shorter than 400 nm, are of extreme interest because of their current applications and future prospects of newer and improved applications. Currently, the market size of UV business is more than US$500 million (Micronews, 2009) with traditional UV lamp technology, such as mercury vapor lamps. Owing to its compactness, lower cost, and environmental friendly composition, UV LEDs are expected to replace traditional lamps and also will pave the way for opening up many new applications, especially portable ones.

The III-nitride semiconductor devices were first commercialized only in 1992, much later than other conventional semiconductors, such as silicon and GaAs. The main causes for the delay in their development were the lack of suitably lattice-matched substrates and the difficulty of incorporating nitrogen into the III-nitride semiconductors. In addition to that, the electrical conductivity of III-nitride materials was uncontrollable due to their poor crystal quality and this effectively prevented the researchers from fabricating high-performance devices that can lead to commercialization for a long period of time. In the mid-1980s, experimental procedures were developed that enabled the growth of high-quality single-crystal materials of binary and ternary III-nitride semiconductors, such as GaN, InGaN, and AlGaN, by using low-temperature (LT) nucleation layers of either AlN (Amano *et al.*, 1986) or GaN (Nakamura, 1991). Another extremely significant development that followed was the realization of p-type GaN using low-energy electron-beam irradiation (LEEBI) (Amano *et al.*, 1989) and subsequently by thermal annealing (Nakamura *et al.*, 1992). These major breakthroughs paved the way for the development of commercial III-nitride-based visible and long-wavelength UV optical devices. However, since the first commercialization of III-nitride devices, their subsequent development has been phenomenal as evidenced by the fact that the market size for GaN-based devices (mainly high-brightness LEDs) alone was US$4.6 billion in 2008 (Strategies Unlimited's Report – PennWell Corporation, 2009).

With the visible- light-emission device technology sans green reaching its maturity, the major focus has been shifted toward achieving better- performance shorter-wavelength UV and green devices. The interest in short-wavelength UV devices is ignited by the potential applications for the UV LEDs in air and water purification, germicidal and biomedical instrumentation systems, and for the UV LDs in medical surgery and other uses (Khan *et al.*, 2005). The quantum efficiency of the near-UV LED received a huge boost with advanced growth, metallization, and packaging techniques. The emission wavelengths of LEDs now cover the majority of the UV spectrum ranging from 400 to 210 nm (Khan *et al.*, 2008). UV laser diode emission has shifted toward shorter wavelengths with viable operation demonstrated down to 342 nm. The UV part of the electromagnetic spectrum lies in the wavelength range 10–400 nm. The UV spectrum is classified into four distinct regions: UV-A or long-wave UV (320–400 nm), UV-B or mid-wave UV (290–320 nm), UV-C or short-wave UV (200–290 nm), and vacuum UV (10–200 nm). III-nitride-based LEDs have the theoretical capability to emit at all wavelengths in the UV-A, -B, and -C, with 210–400 nm LEDs already demonstrated. The emission wavelength is dictated by the fundamental band gap of the material used in the active region of the device, with AlN having a band gap of 6.2 eV at room temperature (RT) corresponding to an emission wavelength of approximately 210 nm; GaN to a wavelength of 365 nm; and low indium composition InGaN having a band gap corresponding to an emission wavelength of approximately 400 nm. The UV-B and UV-C wavelength regions are commonly referred to as the deep UV (DUV) regime.

DUV light-emitting devices offer a variety of options, primarily due to the interaction between UV radiation in this wavelength regime and biological species, including high-density optical storage, efficient white LEDs, water and food sterilization, portable biological and chemical agent detection systems, non-line-of-sight communication (NLOS), industrial spot curing, hardening or curing resins as part of the assembly process of plastic lenses in digital cameras and optical pickups in digital video disks (DVDs) and compact disks (CDs), counterfeit currency detection, credit card checking, and security inks. It must be also mentioned that the absorption of radiation by the atmospheric ozone is very strong for UV wavelengths shorter than ~280 nm, resulting in very little solar radiation in this wavelength regime being present near the earth's surface. Hence, biological organisms on earth have never developed a tolerance for this radiation. Therefore, man-made UV-C light source has become a vital tool in the treatment and destruction of bacteria, yeast, viruses, and fungi. Mercury, xenon, and deuterium lamps with emission spectra ranging from 254 to about 290 nm have been used extensively for purification of microbiological contaminants in air and water. However, their high operating voltages and larger size, together with the environmental hazards of using mercury, preclude their use in techniques for disinfection, air and water purification, and in biomedicine. In addition to that, these sources have relatively shorter lifetimes when compared with III-nitride-based UV emitters, lack of wavelength choices or tuneability, power modulation difficulty, environmental pollution, and a few other disadvantages make them worthless to persist with. Replacement of these conventional sources with III-N semiconductor detectors will solve most of these problems and offer several additional advantages, including miniaturization, reliability, reduced costs, low power consumption, and, ultimately, a choice of wavelength of operation between 365 and 200 nm. **Figure 1** presents some applications requiring UV radiation, such as industrial spot curing (a), treatment of psoriasis by UV phototherapy (b), and air and water purification (c).

This chapter discusses the current status and the evolution of III-nitride-based short-wavelength UV light emitters under two broad sections: long-wavelength UV LEDs (covering UV-A LEDs) and DUV LEDs (covering both UV-B and UV-C LEDs). Since device operation in the DUV region primarily requires AlGaN-based active layers with very high Al molar fraction in the alloy, some pertinent material issues and challenges in the material growth are discussed. The problems of strain, cracking, and defects in AlGaN layers heteroepitaxially grown over sapphire substrates are included. Problems of doping of AlGaN are also covered along with the discussion of the AlGaN band-gap bowing. In the final section of the chapter, the development of UV LD is discussed.

6.01.2 Long-Wavelength UV LEDs

The technology for the long-wavelength or UV-A light emitters with emission at wavelengths longer than 365 nm is fairly well established as it was developed simultaneously with the visible blue–green

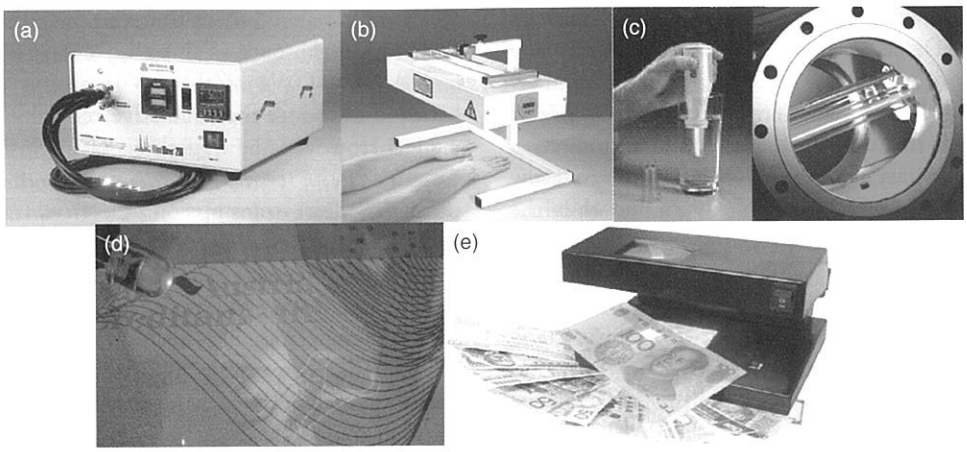

Figure 1 Applications requiring short-wavelength ultraviolet (UV) and deep-(D)UV radiations. (a) Industrial spot curing, (b) treatment of psoriasis by UV phototheraphy by a 308-nm lamp, (c) air and water purification, (d) currency counterfeit detection, and (e) credit card detection. (e) From Lingyunxin Group Co., Ltd.

light emitters. Due to the similarity in recombination mechanisms and device design with visible light emitters, the UV-A devices were relatively easier to manufacture when compared with the DUV devices. The 365–400-nm emission LEDs are now widely available, with most of the commercially available devices utilizing InGaN quantum-wells (QWs). UV-A devices on GaN substrates exhibit increased efficiency compared with the devices grown on sapphire. This is a result of the reduction in the threading dislocation density (TDD) because of using the low dislocation density native bulk or quasi-bulk substrate material. In addition to the TDDs, as the emission wavelength approaches 365 nm, GaN and, particularly, p-type GaN, becomes absorbing which can greatly affect the extraction of light from the semiconductor chip. Morita *et al.* (2002) have developed 365-nm LEDs with a GaN-free device structure that is achieved through laser-assisted liftoff/separation of the GaN from the sapphire substrate, followed by removal the of the exposed GaN. This resulted in 365-nm LEDs with external quantum efficiencies (EQEs) in excess of 5%, despite being grown initially using a conventional metal-organic chemical-vapor deposition (MOCVD) GaN on sapphire growth approach. Subsequently, it has been demonstrated that utilizing the same approach (substrate and GaN removal), but on GaN substrates, resulted in increased efficiency and device lifetime compared to devices grown on several microns of GaN on sapphire due to the lower TDD from the starting bulk GaN material. These devices are now commercially available and large power chips (~1 mm × 1 mm) offer 250 mW of continuous wave (CW) output power at 365 nm with an injection current of 500 mA, corresponding to EQE of 14.7%. Smaller conventional-size LED chips are available in wavelengths ranging from 365 to 395 nm with typical output power at 20 mA ranging from 2 to 10 mW.

The UV-A LEDs with emission wavelengths less than 365 nm require AlGaN active regions and, to date, these have not achieved the same efficiency as the GaN/InGaN LEDs. Various methods were adopted to achieve LEDs with emission wavelengths below 365 nm (the band edge of GaN). The first GaN–AlGaN multiple QW (MQW) with emission at 330–365 nm was demonstrated by Khan *et al.* (1990). The UV-A emission was achieved by changing the transition energy through quantum confinement in the GaN QWs. This is similar to the approach used to fabricate 365-nm LEDs with $In_{0.01}Ga_{0.99}N$ QWs. Subsequently, Han *et al.* (1998) used an $Al_{0.2}Ga_{0.8}N/GaN$ MQW structure to achieve the emission at 353 nm. An output power of 13 μW at 20 mA was achieved, and the corresponding EQE was much less than 1%. To shift the emission wavelength below 350 nm, several groups employed $Al_xGa_{1-x}N/Al_yGa_{1-y}N$ MQWs (Nishida and Kobayashi (1999); Kinoshita *et al.*, 2000) or a double heterostructure (DH) active layer (Otsuka *et al.*, 2000). Another approach used to achieve shorter-wavelength emission was the utilization of quaternary AlInGaN employed by Khan *et al.* (2000). As the presence of indium in the active regions of visible LEDs leads to greatly improved efficiencies, attempts

have been made to include small amounts of indium in UV LEDs as well. Subsequently, 340 nm and shorter-wavelength UV-A LEDs were achieved by using the AlInGaN quaternary epilayers. Several other groups had demonstrated that the introduction of In into ternary AlGaN alloys could improve the optical quality of the AlGaN layers and thus the optical and electrical properties of the LEDs (McIntosh *et al.*, 1996; Hirayama *et al.*, 2001; Han *et al.*, 2000; Hirayama *et al.*, 2002). The quaternary AlInGaN MQW active region was grown using pulsed atomic-layer epitaxy (PALE), which has been shown to result in better quality of the material in the quaternary layers because the PALE method gives better control of the composition and surface morphology (Zhang *et al.*, 2001a, 2001b). Kinoshita *et al.* (2000) reported an LED on SiC with emission at 333 nm by incorporating a Mg-doped $Al_{0.25}Ga_{0.75}N$/GaN superlattice (SL) similar to that of Nishida *et al.* (2000). The SL was claimed to improve the hole injection into the active region. For all these developments on UV-A LEDs, the emission intensity was considerably lower than that of the III-nitride visible LEDs with InGaN–GaN QWs in the active region.

6.01.2.1 Reasons for Poor Efficiency of UV Light Emitters

The low efficiency of the UV light emitters, especially DUV devices, is believed to be caused by some prominent factors, namely, quantum-confined Stark effect (QCSE), poor alloy clustering, low carrier confinement, and absorbing p-GaN contact layers.

The QCSE is caused by the strong spontaneous and piezoelectric fields in the QWs composed of III-nitride materials (Lefebvre *et al.*, 1999; Waltereit *et al.*, 2000). For the III-N materials, these fields become stronger with increasing aluminum alloy compositions that are needed for the UV emission devices. These electric fields lead to reduced radiative recombination efficiency. The QCSE bends the semiconductor valence and conduction bands, leading to a physical separation of the electron and hole pairs. This reduces their recombination probability in the QWs, which, in turn, leads to reduced emission efficiencies (Bernardini *et al.*, 1997).

Poor alloy clustering was believed to be the reason for the unusually high emission efficiency for visible emitters, given the relatively large TDD ($>10^8$ cm^{-2}) in the active region. Formation of indium-rich clusters physically confined the carriers in the InGaN–GaN QWs and separated them from the threading dislocations (TDs). Absence of this alloy clustering in GaN and AlGaN QWs of the UV emission devices is believed to reduce their radiative recombination efficiency. However, the hypothesis of In clustering was disputed more recently by Smeeton *et al.* (2006) through their transmission electron microscopy (TEM) analysis results (Smeeton *et al.*, 2006). The TEM measurements performed on samples under various incident electron beam (e-beam) dosages showed a correlation between their measurement conditions and the observed alloy clustering. Based on this new finding, continued exploration of recombination physics for both InGaN/GaN QWs and their AlGaN/AlGaN UV counterparts is necessary to determine whether there are any fundamental differences in the active regions of visible and UV LEDs and their respective recombination mechanisms.

Low carrier confinement in the active region of the UV and DUV light emitters is one of the major causes why their efficiencies are considerably inferior when compared with their visible counterparts. Early reports of UV LEDs commonly showed multiple emission peaks at long wavelengths, indicating loss of carriers to regions other than the active region and, hence, unintended radiative transitions. At that time, it was unclear whether this resulted from deep-level transitions in the QWs, or from recombination occurring outside of the active region. It was, however, observed that the addition of p-type AlGaN above the QWs reduced the intensity of the deep-level peaks, indicating that the deep level resulted from electrons passing through the active region and recombining with holes in the p-type material (Otsuka *et al.*, 2000). Confinement of the electrons using a higher aluminum composition AlGaN electron-blocking layer between the QWs and p-type contact layer was determined to be more critical than efforts to confine holes using a similar hole blocking layer between the QWs and the n-AlGaN contact layer, due to the low mobility and injection efficiency of the holes compared to electrons. Similar electron-blocking layers are commonly used for blue InGaN/GaN LEDs and laser diodes to avoid long-wavelength emission.

Absorbing p-GaN contact layers used in the UV emitters with emission wavelengths less than 365 nm considerably reduces their efficiency. This problem is more severe for the DUV devices. In addition, UV emission from the active region is absorbed by the thin metal contacts used in the devices. UV-absorbing substrates, such as GaN and SiC,

when used, also cause absorption problems for the devices. Although substrate absorption limited the extraction efficiency of the early devices, several groups were able to demonstrate that defects in the material also greatly decrease the efficiency of these devices and obtain reasonable output power even for devices grown on absorbing substrates. A 352-nm LED with EQE of 1% was measured for a device grown on a free-standing GaN substrate, with typical dislocation density of $\sim 1 \times 10^6$ cm^{-2} (Motoki *et al.*, 2001). Edmond *et al.* (2004) also demonstrated 340-nm LEDs with an EQE of 4% grown on absorbing SiC by implementing a broad-area defect reduction (BADR) growth technique by which silicon nitride defect masks are deposited on the surface in a random orientation to block crystalline defects from propagating into the active region of the LED (Edmond *et al.*, 2004). This work demonstrated the potential for much higher-power UV emitters due to current limitations both with internal and extraction efficiency of the devices. Despite the still relatively low quantum efficiency, compared with visible LEDs, UV-A LEDs are starting to find applications in fluorescence spectroscopy, and industrial curing (Jeys *et al.*, 2003; Jeon *et al.*, 2004).

Enhancing light extraction from an LED is an important factor to improve the device performance. The low light extraction from a nitride-based LED is caused by the large difference in refractive indices between the GaN (refractive index is 2.5) and the air space (refractive index is 1). Due to this, a major portion of the light generated in the active layer of the LED is reflected back in to the device. Various methods have been employed to reduce the problem of light trapping in the DUV LEDs. Oder *et al.* (2003, 2004) achieved an increase of 340-nm LED output power using photonic crystals. The optical power was reported to increase from 44.5 to 86.6 μW. Khizar *et al.* (2005) reported on the fabrication of 280-nm AlGaN-based DUV LEDs on sapphire substrates with an integrated microlens array. Microlenses with a diameter of 12 μm were fabricated on the sapphire substrate by resist thermal reflow and plasma dry etching. LEDs were flip-chip bonded on high thermal conductive AlN ceramic submounts to improve the thermal dissipation, the emitted UV light was extracted through the sapphire substrates, and 55% increase of output at 20 mA direct current (DC) driving was reported. Khan (2006) reported the development of UV transparent planar Fresnel microlenses over sapphire substrates. These lenses were formed on sapphire using a SiO_2-based coating material patterned by direct e-beam writing. Vertical step-like profile of each ring was achieved through multiple exposures so that each ring had a maximum thickness of 560 nm graded in four steps to zero thickness. Lens design was optimized for 280-nm wavelength with 4π maximum phase shift and it was found to work well for a visible LED providing 2π maximum phase shift.

6.01.3 DUV Light-Emitting Devices

As described in the initial part of this chapter, there are strong reasons for desiring the development of solid-state devices emitting in the DUV region. The key events related to the development of DUV light-emitting devices are presented in **Table 1**

The primary difference between UV-B/C devices and the previously discussed UV-A devices is that it was no longer possible to use a GaN-based layer, as was commonly used for the UV-A devices, due to the much larger tensile strain that results for AlGaN grown on GaN. This leads to cracking of the AlGaN films and catastrophic failure for LED devices. Increasing the aluminum composition (needed for the DUV devices) also leads to difficulties in the growth of high structural quality material, typically resulting in an even higher dislocation density for AlGaN alloys compared to GaN. It also leads to difficulties in doping the material to impart it n-type and p-type conductivity.

6.01.3.1 Growth of $Al_xGa_{1-x}N$

In order to fabricate DUV light emitters, low-defect-density AlN and AlGaN materials are needed. The growth of $Al_xGa_{1-x}N$ has proved to be significantly more difficult when compared with that of GaN. This problem is partially due to the fact that Al-adatoms have a much larger sticking coefficient than Ga-adatoms. It is well known that layer-by-layer growth of films with attachment of adatoms at steps or kinks gives the smoothest surface features, as opposed to three-dimensional island growth. As Al-adatoms have a low mobility on the surface, they are less likely to be able to move from their point of impact from the vapor and, rather than incorporating at the most energetically favorable lattice sites such as at a step, they tend to cause islands to nucleate which disturb the epitaxial growth. As a result, higher densities of extended defects, such as dislocations and grain boundaries, are much easier to generate as these growth islands from

Table 1 Summary of the major developments that took place during the development of III-nitride-based UV emitters

Significant developments	*Researchers (year)*
First single-crystal GaN on sapphire	Maruska and Tietjen (1969)
First GaN-based MIS LED	Pankove *et al.* (1971)
Low-temperature AlN buffer layer	Amano *et al.* (1989)
First p-n junction GaN blue LED	Amano *et al.* (1989)
AlgaN–GaN–AlGaN MQW	Khan *et al.* (1990)
p-Type GaN by low-energy electron-beam irradiation (LEEBI)	Amano *et al.* (1990)
Low-temperature GaN buffer layer	Nakamura *et al.* (1991)
AlGaN/GaN MQW LED	Han *et al.* (1998)
Smooth AlN with low V/III ratio	Ohba *et al.* (1996 and 2001)
352-nm LED on bulk GaN	Nishida *et al.* (2001)
340-nm UV LED	Adivarahan *et al.* (2001)
315-nm LED	Khan *et al.* (2001)
305-nm UV-LED	Khan *et al.* (2001)
AlN/AlGaN SL for thick and crack-free n-AlGaN	Zhang *et al.* (2001)
UV-LED 285 nm	Adivarahan *et al.* (2002)
GaN-free UV LED (365 nm)	Morita *et al.* (2002)
280-nm LED	Yasan *et al.* (2002)
365-nm-laser diode (cw)	Masui *et al.* (2003)
359.7-361.6-laser diode (pulsed)	Kneissl *et al.* (2003)
354.7-nm-laser diode (pulsed)	Masui *et al.* (2003)
350.9-nm-lased diode (cw)	Iida *et al. et al.* (2004)
348-nm-laser diode (cw)	Edmond *et al.* (2004)
343-nm-laser diode (pulsed)	Edmond *et al.* (2004)
342-nm-laser diode (pulsed)	Yoshida *et al.* (2008a)
336-nm-laser diode (pulsed)	Yoshida *et al.* (2008b)
269-nm LED	Adivarahan *et al.* (2004)
254-nm LED	Wu *et al.* (2004)
250-nm LED	Adivarahan *et al.* (2004)
210-nm AlN LED	Taniyasu *et al.* (2006)
Stimulated emission from AlN at 214 nm	Shatalov *et al.* (2006)
High-temperature AlN growth (1500 °C)	Balakrishnan *et al.* (2006)
MOHVPE AlN growth	Fareed *et al.* (2006)
Vertically conducting deep-UV LED	Adivarahan *et al.* (2009)

different nucleation sites coalesce. Moreover, in the MOCVD growth of $Al_xGa_{1-x}N$ layers, the commonly used Al-metalorganic precursors (trimethylaluminum (TMA) and triethylaluminum (TMG)) are known to be more reactive than their Ga-based counterparts. Hence, gas-phase reactions and related adduct formations tend to interfere with the growth process. **Figure 2** presents an experimental plot for Al incorporation in the solid film as a function of the Al fraction in the gas phase (Khan *et al.*, 2006). Under such growth conditions, the Al incorporation is very efficient when the gas-phase fraction is smaller than 50% (molar fraction: TMA/(TMA+TMG)). Above 50%, a reduced level of incorporation has been observed due to the gas-phase reaction between TMA and NH_3. This reaction could interrupt the normal epitaxial growth process by generating nano- or micro- particles which fall onto the growing surfaces. As a result, for high-Al-content AlGaN, to avoid surface roughening, pits and particles, and associated structural defects, a lower growth rate must be employed. Other critical problems affecting epitaxial growth of high-quality AlGaN films include film cracking and poor electrical conductivity. These factors present great challenges for device-development efforts, and require a full exploration of the materials deposition domain for AlGaN, including the introduction of extensive innovative approaches. Some of the major approaches attempted to resolve these problems are now presented.

Recently, there have been major developments in the production of native substrates, including GaN, AlN, and their alloys, as free-standing wafers using a variety of growth techniques (Bockowski *et al.*, 2004; Zhang and Meyer 2003; Rojo *et al.*, 2001; Kim *et al.*, 1998). However, the stage has not reached where these substrates of consistently high quality and size

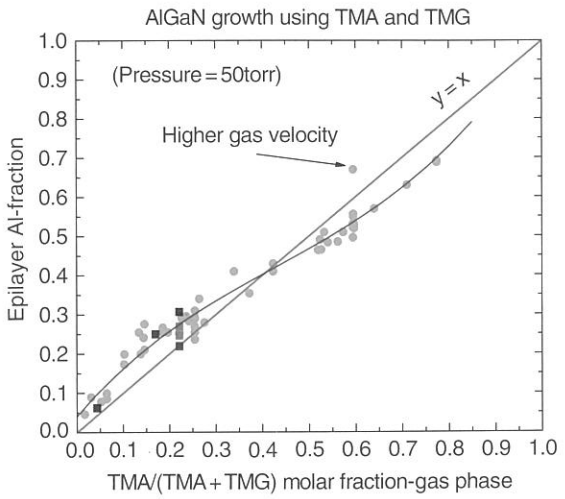

Figure 2 Al composition in the AlGaN layers as a function of Al fraction in the gas phase. Under the used growth conditions, Al incorporation is efficient when the Algas fraction is less than 50%. Above 50%, a reduced Al composition in solids compared to gas phase indicates a pronounced gas-phase reaction has occurred. High gas velocity (including lower growth pressure and high push gas) could increase Al incorporation.

required for the commercial device production are available. Due to this reason, nitride thin films tend to be grown on foreign substrates, a process known as hetero-epitaxy. Commonly used substrates include sapphire (Al_2O_3), SiC, Si, and GaAs. For each foreign substrate, there are differences in the lattice parameters and the thermal expansion coefficients compared with the nitride materials. In addition to the formation of TDs, the nitride films tend to be bowed and even cracked. The usefulness of LT buffer layers for improving the quality of hetero-epitaxial GaN films has been recognized since 1986 (Amano *et al.*, 1986). As the problems with AlGaN films are even more severe, researchers have developed novel approaches based on the idea of compliant-layer insertion. Kamiyama *et al.* (2001) and Han *et al.* (2001) individually adapted LT AlN and AlGaN insertions to avoid cracking of AlGaN grown on GaN. The periodic insertion of LT-grown AlGaN layers was shown to effectively reduce the biaxial tensile strain in the AlGaN films, thus reducing the cracking (Han *et al.*, 2001). The LT-grown films tend to exhibit poorer structural quality and, hence, to possess less stiffness. The LT films are more elastic, making them more compliant and able to accommodate more strain. However, this method could still introduce dislocations after each LT-layer insertion. Besides, there are too many thermal cyclings during one growth, which also makes the technique less attractive.

An alloy composition with a low V/III ratio (about 1:4) and high growth temperatures in the order of 1200 °C were used to achieve a two-dimensional growth mode for AlN on sapphire substrates. The cracking of AlGaN films grown on basal plane sapphire substrates is surprising because from the lattice and thermal mismatch point of view, AlGaN grown on sapphire should experience biaxial compressive strain, which could not cause cracking at all. The strain responsible for this kind of cracking is rooted in a different mechanism and is called 'intrinsic tensile strain', often observed in imperfect materials (polycrystalline) growth. It arises from the coalescence of islands where the film consists of discrete mosaic blocks. During growth when two islands (mosaic blocks) begin to approach each other at a certain distance, they will begin to coalesce through atomic rearrangement to allow a minimized system free energy by reducing two surface boundaries to one. This process, however, will generate tensile strain in the vicinity of the zipped area, and the strain is inversely proportional to the square root of the island dimension (Gao and Nix, 1999). The energy from the tensile strain will therefore build up with film thickness, to a point where it will be released either by dislocation generation or by cracking. Cracking is likely to happen in a material system where dislocations have no slip system, as in AlGaN films. AlGaN films grown on sapphire consist of many fine mosaic blocks and the coalescence of these mosaic blocks will generate intrinsic tensile strain; therefore, eventually the film must crack. This kind of cracking can be avoided by improving the material quality, that is, by decreasing the material mosaicity (increasing the mosaic block dimensions). It has been suggested by Khan *et al.* (1992a, 1992b, 1993) that the PALE approach could be used to grow high-quality AlN and AlGaN films. In the PALE approach, the flow rates of group III and group V precursors are sequentially modulated, enhancing surface migration of Al- and Ga-adatoms, which results in better crystalline quality and surface morphology of epitaxial layers. Another approach was suggested by Bykhovsky *et al.* (1997) who theoretically predicted elastic strain relaxation in GaN/AlN and GaN/AlGaN SLs. Zhang *et al.* (2002a, 2002c) has reported on using AlN/AlGaN SLs for alleviating the crack problem of thick AlGaN films over sapphire substrates, and Wang *et al.* (2002)

noted that detailed X-ray measurements indicated that these SLs were efficient in enhancing AlGaN mosaic block dimensions. Later, a modified PALE approach, known as the migration-enhanced metal-organic chemical-vapor deposition (MEMOCVD) technique, was employed to further enlarge the AlGaN mosaic block dimensions (Zhang *et al.*, 2002b). In the MEMOVD method, the duration of the group III and group V precursor pulses is further optimized in a pattern that allows beneficial surface migration of the reacting species on the growing film. This allows changing the V/III ratio from vanishingly small to several thousands, which greatly increases the probability that the Al- and Ga-adatoms migrate to their appropriate sites in the lattice. Very-high-quality AlN and AlN/AlGaN SLs were grown by this method.

AlGaN device structures grown over these MEMOCVD AlN and AlN/AlGaN SLs were also measured to be of superior quality, in terms of structural quality and minority carrier lifetime (Mickevicius *et al.*, 2005). **Figure 3**(**a**) presents the scanning electron microscope (SEM) image of a cracked AlGaN layer grown on a sapphire substrate with an

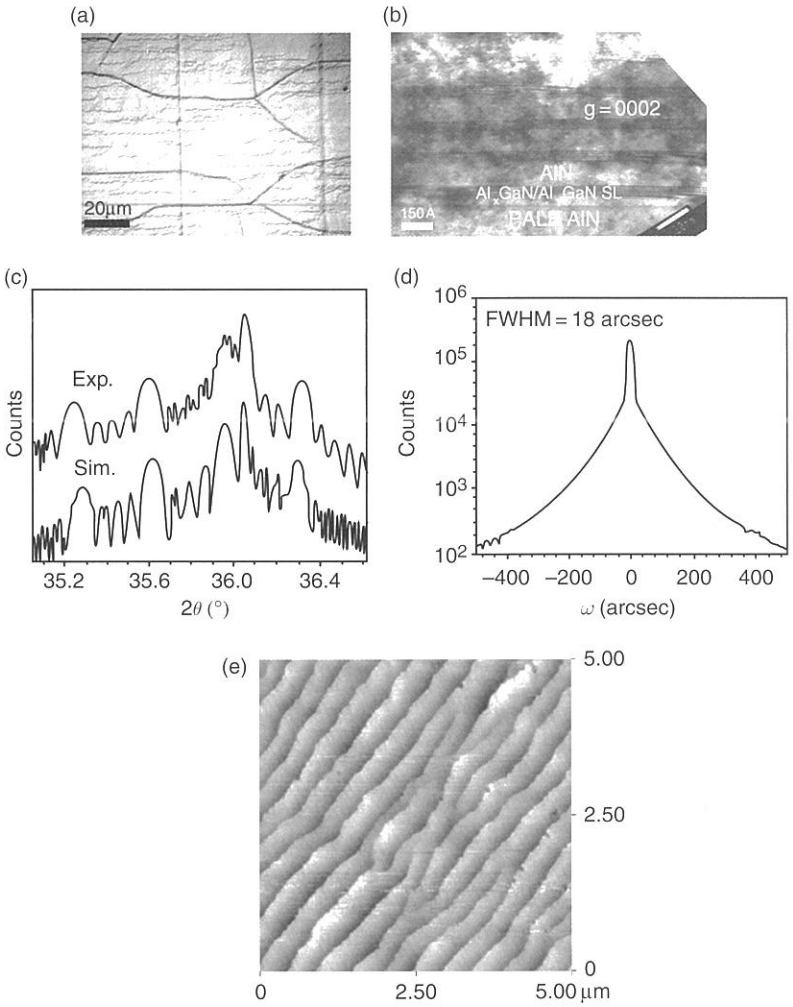

Figure 3 (a) Scanning electron microscope (SEM) image of a cracked AlGaN layer grown on a sapphire substrate with an AlN buffer layer. (b) Cross-sectional transmission electron microscope (TEM) image of a pulsed atomic-layer epitaxy (PALE)-grown AlN on sapphire with the $Al_xGa_{1-x}N/Al_yGa_{1-y}N$ strain-relief superlattice that enables the growth of thick n-type AlGaN. (c) Experimental and (d) simulated (0002) X-ray diffraction (XRD) 2θ–ω spectra for $AlN/Al_{0.85}Ga_{0.15}N$ supperlattice layers. (e) Atomic force microscope (AFM) image of PALE grown AlN layer on sapphire substrate with $Al_xGa_{1-x}N/Al_yGa_{1-y}N$ strain-relief superlattice. (c, d) Reproduced from Zhang JP, Khan MA, Sun WH, *et al.* (2002) Pulsed atomic-layer epitaxy of ultrahigh-quality $Al_xGa_{1-x}N$ structures for deep ultraviolet emissions below 230 nm. *Applied Physics Letters* 81: 4392–4394, with permission from American Institute of Physics.

AlN buffer layer. **Figure 3(b)** shows a cross-sectional transmission electron microscope (TEM) image of a PALE-grown AlN on sapphire with the $Al_xGa_{1-x}N/Al_yGa_{1-y}N$ strain-relief SL that enables the growth of thick n-type AlGaN. **Figures 3(c)** and **3(d)** show the experimental and simulated (0002) X-ray diffraction (XRD) 2θ–ω spectra for $AlN/Al_{0.85}Ga_{0.15}N$ SL layers, respectively. **Figure 3(e)** presents an atomic force microscopy image of PALE-grown AlN layer on sapphire substrate with $Al_xGa_{1-x}N/Al_yGa_{1-y}N$ strain-relief SL. Development of the AlGaN/AlN SL buffer layers enabled growth of highly doped n-AlGaN to a thickness of greater than 2.0 μm, enabling the development of UV-B and UV-C devices with submilliwatt- and, later, milliwatt-level output powers (Sun *et al.*, 2004; Zhang, 2004).

There are also several other approaches that have been explored to improve AlGaN quality. Kamiyama *et al.* (2002) used grooved GaN templates for AlGaN growth with the aim of bending the TDs away from the growth direction. A similar method, which uses GaN templates and air-bridged lateral growth of AlGaN, had also been demonstrated (Kawaguchi *et al.*, 2003). One limitation to those approaches is that they are only efficient in low Al-content AlGaN growth. These methods encounter difficulties in high-Al-content materials because of the very small lateral growth rate. Pioneering work on epitaxial growth and characterization of AlN and AlGaN layers over bulk AlN substrates was reported by several groups (Gaska, *et al.*, 2002; Rojo *et al.*, 2002; Hu *et al.*, 2003; Nishida *et al.*, 2004; Silveira *et al.*, 2004). Numerous advantages of bulk AlN substrates, such as possibility of homoepitaxial growth, potential transparency in the UV region, high thermal conductivity, have been addressed. Widespread commercial availability of these bulk substrates of uniform quality can be expected to provide the ultimate solution for growth of crack-free high-quality AlGaN films.

More recently, high-temperature growth by the MOCVD method has been employed successfully to grow AlN layers with better structural quality. By the conventional MOCVD growth, the maximum growth temperature employed is around 1200 °C. In the high-temperature methods, temperatures in the range of 1200–1600 °C are used. The high-temperature condition is expected to promote two-dimensional growth in the case of III-nitride semiconductors, especially AlN, as it causes increase of the diffusion length of cation species. Balakrishnan *et al.* (2007) have investigated the AlN growth on SiC under high-temperature conditions up to 1500 °C and reported that their resultant layers contained a dislocation density as low as 10^6 cm^{-2} (Chen *et al.*, 2006). Similarly, the high-temperature growth technique has been successfully employed to grow AlN and AlGaN layers on other substrates as well, and, in many cases, crack-free layers with high structural quality of thickness more than 6 μm have been reported (Imura *et al.*, 2006a, 2006b; Okada, *et al.*, 2006; Imura *et al.*, 2007; Okada *et al.*, 2007; Kato *et al.*, 2007).

This was followed by another novel approach used to grow AlN films in order to combine MOCVD and hydride vapor-phase epitaxy (HVPE) in a single growth chamber (Fareed *et al.*, 2007). This has been found to be effective to deposit 20-μm-thick, crack-free single-crystal AlN films over grooved basal plane sapphire substrates with lateral growth rates in excess of 2 mm h^{-1}. This approach, where MOCVD and HVPE growths can be carried out in the same reactor either sequentially or simultaneously in any arbitrary order, is referred to as 'metal-organic hydride-vapor-phase epitaxy' (MOHVPE). The combination of MOCVD and HVPE in the same reactor affords the flexibility to grow buffer and device layers at growth rates ranging from 0.1 to 10 mm h^{-1} without removing the substrate. It is therefore ideal for the deposition of thick AlN buffers and DUV light-emission devices over substrates such as sapphire with excellent optical properties but a low thermal conductivity. In addition, the viability of the MOHVPE process for fast lateral epitaxy of AlN and a subsequent growth of high-quality UVC LED epilayers was demonstrated for the first time.

6.01.3.2 Energy Gap Bowing in $Al_xGa_{1-x}N$ materials

It is important to know the fundamental band gap of AlGaN over a large range of Al mole fractions in the design of UV light-emitting devices. The results of absorption measurements performed at atmospheric pressure yielded the variation of the band-gap energy which was found to be $E_g(x) = 3.43 + 1.44x + 1.33x^2$ eV for the $Al_xGa_{1-x}N$ system (Shan *et al.*, 1999). There is a large nonlinear variation with concentration for the fundamental band gap. When the experimental bowing parameter of 1.0 is used, the relationship obtained is $E_g(x) = 6.2x + 3.43\ (1 - x) - x\ (1 - x)$, and this has been generally adopted (Malikova *et al.*, 1997).

6.01.3.2.1 Doping of $Al_xGa_{1-x}N$ materials

6.01.3.2.1(i) n-Type doping The doping of AlGaN materials is still not established to the extent of the doping in GaN and InGaN. There is a rapid decrease in the conductivity for both doping types with increasing Al compositions. As the aluminum composition is increased, the band gap of the $Al_xGa_{1-x}N$ semiconductor increases and the ionization energies for silicon (most commonly used n-type dopant) and magnesium (most commonly used p-type dopant) increase, resulting in a lower ionization efficiency. In addition, the material quality is degraded with the increase of dopants and this causes poor mobility of carriers in the lattice. $Al_xGa_{1-x}N$ materials with low resistivity are specifically desired because most DUV light emitters are prepared on transparent sapphire, with a few initial demonstrations using bulk and pseudo-bulk AlN substrates. Both sapphire and AlN are electrically insulating and thus necessitate the fabrication of laterally conducting light-emitting devices with both contacts on the same side of the wafer. Higher resistivity of the n-contact AlGaN layer results in nonuniform current injection in the light-emitting device active area, known as 'current crowding', which leads to increased injection currents along the perimeter of the LED mesa (Guo and Schubert, 2001).

As mentioned above, the MEMOCVD growth method has been shown to produce high-quality AlN and AlN/AlGaN SLs for defect reduction in AlGaN and such defect reduction can greatly improve the doping efficiency by reducing compensating and scattering centers. As a result, RT electron Hall mobilities exceeding 85 $cm^2\ V^{-1}\ s^{-1}$ for n-AlGaN with Al molar fraction of 50% have been obtained (Zhang *et al.*, 2003). Using molecular beam epitaxy (MBE) Si doping in high-Al-mole fraction AlGaN alloys has been achieved with very high n-type carrier concentrations $\sim 10^{20}\ cm^{-3}$, but with poor mobility (Hwang *et al.*, 2002). No significant degradation of materials properties was reported. Si δ-doping, where basically an atomic plane of Si atoms was introduced as the electron source, has been introduced for a 340-nm UV LED structure whereby improved performance with output power of 150 μW at a DC driving current of 100 mA has been achieved (Kim *et al.*, 2003).

6.01.3.2.1(ii) p-Type doping p-Type doping of high Al-content AlGaN is even more challenging as the RT activation energy for the most commonly used acceptor Mg in p-type GaN is already a relatively high 250 meV. It increases for AlGaN such that it is difficult to achieve conduction in p-type AlGaN with aluminum composition greater than ~15–20%. In addition to increasing the device resistance, which results in Joule heating, it is very difficult to make an ohmic contact to p-AlGaN films. Therefore, most researchers deposit a p-GaN film to the top surface to serve as a contact layer, with this film absorbing some of the UV emission. Even if one can inject holes effectively from the metal into the p-GaN material, such holes are then faced with a potential barrier before they can be transported across subsequent AlGaN barrier layers down to the QW. Holes that are trapped at the first interface set up an electric field which can attract electrons to bypass the QWs and hence recombine nonradiatively in the p-GaN layer, having a major impact on quantum efficiency. Several approaches have been suggested to enhance the Mg-doped AlGaN p-type conductivity. One method is to use either a short-period or a large-period superlattice (SPSL or LPSL) composed of Mg-doped AlGaN/GaN layers to replace conventional p-AlGaN (Saxler *et al.*, 1999; Kozodoy *et al.*, 1999; Wang *et al.*, 2002). For the SPSL the period is very small, typically below 4 nm, hence minibands are formed, and vertical conduction of the p-SPSL should not be degraded. In the large period case, the period is typically larger than 15 nm, but the valence band discontinuity as well as the polarization fields can enhance the ionization of the acceptors in the AlGaN barriers and transfer holes into GaN wells. However, since the period is large, wave-function coupling between neighboring wells is forbidden, which greatly reduces the vertical conductivity. As a result, this LPSL approach can only obtain good horizontal p-conductivity. Several groups have used Mg-doped AlGaN/GaN SPSL in 340–350-nm UV LED growth (Kozodoy *et al.*, 1999; Nishida *et al.*, 2001; Peng *et al.*, 2004).

The second approach was proposed by Shur *et al.*, namely, using a p-GaN/p-AlGaN single heterostructure to achieve hole accumulation at the interface (Goepfert *et al.*, 2000; Shur *et al.*, 2000). The mechanism of this approach is similar to the LPSL approach. However, since in the p-GaN/p-AlGaN single heterostructure only one barrier exists for hole transport, the vertical conductivity can be greatly enhanced due to the high-density hole accumulation at the interface and the field assisted tunneling as well as thermionic emission. Most of the reported DUV LEDs used this approach for hole injection into the active layers and obtain reasonably good power (Zhang *et al.*, 2002, 2003; Chitnis *et al.*, 2003; Yasan *et al.*, 2003; Sun, 2004; Adivarahan *et al.*, 2004c; Fischer *et al.*, 2004).

The third approach, δ-doping, has been investigated by Nakarmi *et al.* (2003). It was demonstrated that Mg δ-doping improves not only p-type conduction, but also the overall quality of p-type GaN and AlGaN. It was observed that the Mg δ-doping enhances the hole concentration while inducing no changes in the hole mobility.

6.01.4 Deep-UV (UV-B and UV-C) LEDs

Khan *et al.* reported the first UV-B LED with emission wavelength at 305 nm (Khan *et al.*, 2001). As before, the quaternary AlInGaN MQW active region was grown by PALE. Limitations in material quality, doping problems, and insufficient thickness of the bottom n-AlGaN layers put severe limits on performance due to the high sheet resistance of the n-AlGaN, which immediately created a problem of poor current spreading in mesa geometry devices on sapphire. To overcome the current spreading problem, a stripe geometry configuration was suggested.

The growth of thick (up to 2.5 μm) highly doped n-AlGaN was enabled after the development of novel AlGaN/AlN SL buffer layers (Zhang *et al.*, 2002a), which resulted in a rapid development of improved UV-B LED devices. The submilliwatt operation for an LED with emission at 315 nm and the milliwatt operation for an LED with emission at 325 nm were next reported by Chitnis *et al.* (2002c, 2003a, 2003b). This improvement was achieved by implementing the innovative SL buffer layer approach for growth of low-sheet-resistance n-AlGaN, by optimizing the device geometry for better current spreading, and by introducing flip-chip packaging for improvements in thermal management and light extraction. The problem of lateral current crowding with sapphire-based DUV LEDs has been analyzed and the optimization of the device geometry through the use of an interdigitated multifinger geometry was suggested by Shatalov *et al.* (2002a, 2002b). Optimization of the growth approaches and optimization of the LED structural design along with advanced packaging techniques resulted in milliwatt DC operation of LEDs with the emission at 325 nm as reported by Chitnis *et al.* (2002, 2003a; 2003b). The initial submilliwatt operation of a nitride-based LED emitting in the UV-C band was demonstrated in 2002 by the Adivarahan *et al.* (2002) device, which operated at 285 nm with a CW output power of 10 μW at 60-mA drive current. This device yielded 0.15 mW with 400 mA applied under pulsed conditions. With advancement of contact processing technology, they were able to achieve output power as high as 0.25 mW at 650 mA under pulse-pumping conditions with the next generation of devices. The output power was shown to be thermally quenched by at least 10 times as the operating temperature was raised from 100 K to RT under pulsed conditions. These data indicated that nonradiative recombination at defects rather than a lack of hole transport to the QW is the key contribution to the low quantum efficiency of 285-nm devices. Further optimization of the AlN buffer layer quality by means of PALE has been reported by Zhang *et al.* (2002b, 2003), which enabled improvements in the material quality of the lower n-AlGaN bottom cladding layer as well as the MQW layers, and these advances resulted in a rapid increase of the LED output power up to milliwatt levels (Zhang *et al.*, 2002). By optimization of the quality of the AlGaN layers grown over sapphire substrates, several groups have now reported improved LED devices with emission around 280 nm (Yasan *et al.*, 2002; Zhu *et al.*, 2002, 2003; Hanlon *et al.*, 2003). While the majority of the reports described the optimization of AlGaN growth by MOCVD, others have presented the use of MBE with an ammonia source as an alternative approach, along with innovative short-period SL cladding layers (Kipshidze *et al.*, 2001, 2003; Kuryatkov *et al.*, 2003; Nikishin *et al.*, 2003).

Despite the advancements made in this field, the quantum efficiency of these UV-C LEDs remained much below 1% and worse yet, the emission spectrum consisted of several peaks: a near-band-edge emission from the QW and longer-wavelength peaks associated with deep-level transitions in barrier layers (Zhang *et al.*, 2003; Shatalov *et al.* 2003). This stimulated a second round of device structure and growth optimizations, and many groups reported a significant improvement of device output power and spectral purity (Sun *et al.*, 2004; Mayes *et al.*, 2004; Allerman *et al.*, 2004; Kim *et al.*, 2004). Fischer *et al.* (2004) reported DC power levels as high as 1.34 mW at 300 mA for large-area 290-nm devices, while achieving EQE as high as 0.18% for devices with smaller areas. Later, Sun *et al.* (2004) and Zhang *et al.* (2004) demonstrated high-power UV-C LEDs with emission around 280 nm with DC output power around 1 mW at 20 mA and corresponding EQW of ~1.1%.

UV-C LEDs with emission wavelength in the range of 265–270 nm have also been reported by several groups. Remarkable device performance was achieved by Yasan *et al.* (2003) who reported submilliwatt DC and as high as 4.5-mW pulsed output power at 267 nm corresponding to a quantum efficiency of ~0.1%. These power levels have been further increased by Adivarahan *et al.* (2004) and Bilenko *et al.* (2005), who reported quantum efficiencies of 0.4% and 0.2% at 269 and 265 nm, respectively. Submilliwatt pulsed operation of DUV-C LEDs with emission wavelength as short as 250 nm was reported in 2004 by Adivarahan *et al.* (2004). Subsequently, Allerman *et al.* obtained an electroluminescence peak from a UV-C LED structure at the wavelength as short as 237 nm, demonstrating the possibility for further reduction of emission wavelength toward 200 nm.

The DC operation of LEDs with wavelength shorter than 260 nm becomes severely limited by the lack of conductivity of the bottom Si:doped AlGaN cladding layer since the Al molar fraction required for transparency increases above 70%. To improve the current spreading in LEDs with high Al molar fractions in the AlGaN cladding layers, an interconnected micro-pixel design has been adapted (Adivarahan *et al.*, 2004; Wu *et al.*, 2004). This use of micro-pixels was first introduced for III-nitrides by Mair *et al.* (1997) to improve the light extraction from a AlGaN/GaN slab via the formation of microcavities, and the approach was then used in blue (Jin *et al.*, 2000) and UV-A LEDs (Kim *et al.*, 2003). The micro-pixel LED design was further extended to the formation of photonic crystals (Boroditsky *et al.*, 1999) by the reduction of the size and the period of the array elements (Oder *et al.*, 2003, 2004). An LED design with interconnected micro-pixels separated by the n-AlGaN contact metal was also shown to be very efficient in achieving the desired uniform current pumping for DUV-C LEDs. Devices with emission at 255 nm with 1-mW DC and 3.4-mW pulse power and corresponding maximum quantum efficiencies of 0.14% and 0.3% (in DC and pulse pumping, respectively) were recently demonstrated by Khan *et al.* (2004). Normalized electroluminescence spectra of DUV LEDs are shown in **Figure 4**. All devices exhibit a strong peak corresponding to near-band-edge emission from the MQW active region with full width at the half maximum of about 10 nm. Hence, by proper choice of the AlGaN MQW active region composition, the emission wavelength can be effectively tuned from 255 to 280 nm. The

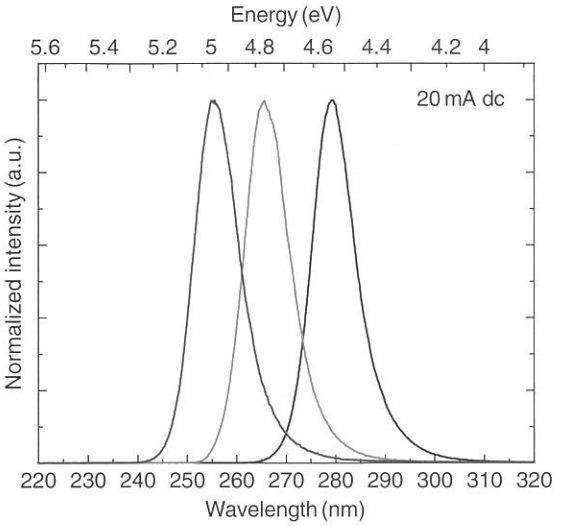

Figure 4 Electroluminescence spectra of deep ultraviolet light-emitting devices (UV LEDs) under 20-mA DC pump current. Reproduced from Khan MA, Shatalov M, Maruska HP, Wang HM, and Kuokstis E (2005) III-nitride UV devices. *Japanese Journal of Applied Physics* 44: 7191–7206, with permission from Japan Society of Applied Physics.

intensity of the main emission peak is stronger than that of long-wavelength emission peaks (at 360–500 nm) by at least 300 times (not shown). Output power versus pump current characteristics for these DUV LEDs are plotted in **Figure 5**. As can be seen in the **Figure 5**, the power (and quantum efficiency) strongly reduces with emission

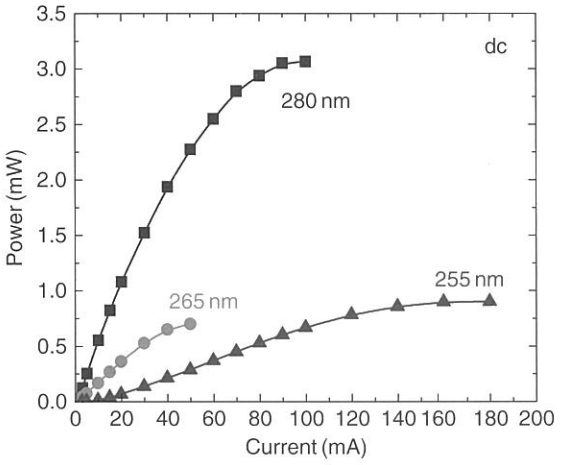

Figure 5 Output power vs. DC pump current characteristics of packaged deep ultraviolet light-emitting device (UV LEDs). Data for 100 μm × 100 μm square device for 280 nm (black) and 265 nm (red) emission LEDs and 10 × 10 micro-pixel array LED for 255 nm (blue) emission LED are shown.

wavelength. This is a consequence of lower doping efficiency and reduced material quality of AlGaN layers with very high Al content. Increasing operation voltage also leads to early power saturation in DC pumping for square geometry devices. Thus, as described above, interconnected micro-pixel array geometry was shown to be an effective solution for devices with shorter emission (i.e., 255 nm). Recently, Deng *et al.* (2007) reported 247-nm DUV LED by employing an MEMOCVD grown structure. The turn-on voltages were lower than 8 V at 20-mA current. Power levels of 0.3 mW were achieved for the packaged devices driven at 90-mA DC current.

Recent efforts on the fabrication of DUV LEDs on pulsed lateral epitaxial overgrowth (PLOG)-grown thick (>15 μm) low-defect AlN buffer layers and by the MOHVPE technique have yielded devices with significant improvement in performance. The excellent thermal conductivity of AlN prevented the devices from premature power saturation. The lower defects and the thick AlN templates resulted in a much superior thermal management, which translated to 280-nm LED lifetimes increasing to well above 2000 h. **Figure 6** presents a typical power density versus current density, measured under DC bias, for a 285-nm LED fabricated by the MOHVPE method. It is very significant that small-periphery MOHVPE LEDs, such as a 50-μm-diameter device, are able to sustain extremely high current densities, up to 4000 A cm^{-2}, without power saturation. This is an indication of the improved thermal dissipation for the LEDs grown on the MOHVPE AlN templates compared to the conventional MOCVD-grown devices. The arrow on **Figure 6** shows the current density for power saturation for a flip-chipped and fully packaged conventional first-generation MOCVD-grown UV LED on a sapphire substrate. The conventional LED output power saturated at approximately 0.5 kA cm^{-2} (delivering an output power density of 3–5 W cm^{-2}) under CW bias condition. It should be noted that for conventional UV LEDs the saturated input current density is increased by about 80% when the devices were flip-chipped to a heat sink and placed on a TO header. The MOHVPE LEDs are expected to handle current densities substantially more than 4.0 kA cm^{-2} after packaging.

Taniyasu *et al.* (2006) have reported the successful control of both n-type and p-type doping in AlN and this allowed them to develop an AlN PIN (p-type/intrinsic/n-type) homojunction LED with an emission wavelength of 210 nm, which is the shortest reported to date for any kind of LED. Their LED structure was fabricated on a SiC substrate.

6.01.4.1 Critical Issues Related with DUV LEDs

Most DUV LEDs are prepared on transparent sapphire substrates, which are totally insulating. The current applied to the DUV LED must be

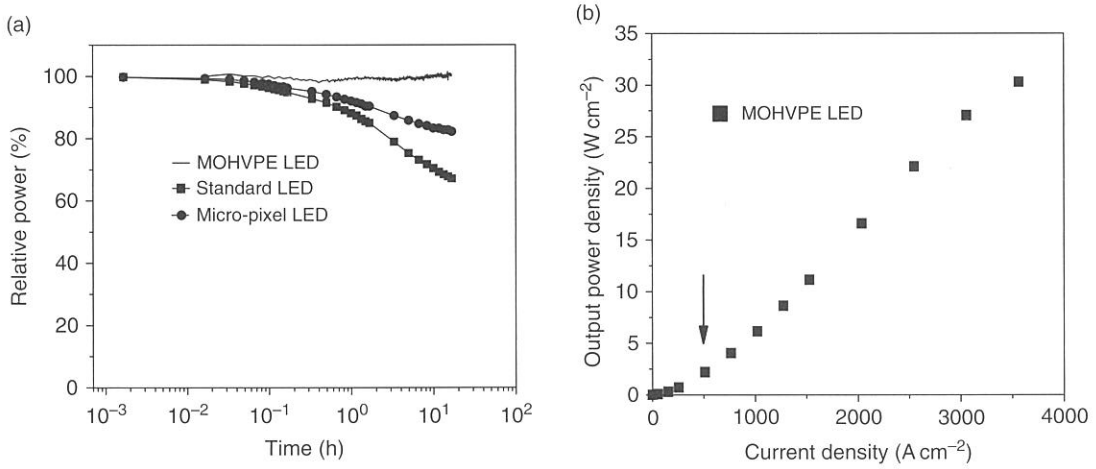

Figure 6 (a). Lifetime reliability of metal-organic hydride-vapor-phase epitaxy (MOHVPE) 280-nm light-emitting device (LED) in comparison with a standard LED and a micro-pixel LED. (b) Comparative continuous-wave (CW) output power density plot of a standard deep-ultraviolet (UV) LED and the LED formed by MOHVPE AlN. Reproduced from Adivarahan V, Fareed Q, Srivastava S, Katona T, Gaevski M, and Khan A (2007) Robust 285 nm deep UV light emitting diodes over metal organic hydride vapor phase epitaxially grown AlN/sapphire templates. *Japanese Journal of Applied Physics* 46(23): 537–539, with permission from Japan Society of Applied Physics.

spread laterally through an n-type AlGaN layer near the substrate, and a high resistivity in such a film limits the extent of current spreading, leading to crowding along the perimeter (Guo and Schubert, 2001). Passage of the current through high-resistance films generates heat. There are even worse problems with p-type AlGaN. The problems associated with p-doping in UV structures are discussed in detail in Section 6.01.3.2.1. Hence, in terms of device performance, these issues create major challenges: uniformity of current spreading, carrier injection, light extraction, and thermal management. These issues are discussed in separate sections subsequently.

6.01.4.1.1 Uniformity of lateral current spreading

In the case of DUV LEDs formed on the electrically insulating sapphire substrates, achieving uniform lateral current spreading is a major issue. This problem has been analyzed and an interdigitated multifinger geometry was demonstrated by Chitnis *et al.* (2003). Using this electrode geometry, the lateral distance between adjacent n-contact metallization is reduced, leading to more spatially uniform current injection throughout the active region of the device. This allows for larger active areas than those permitted by square or circular geometry LEDs. In order to improve the current spreading in LEDs with high Al molar fractions in the AlGaN cladding layers, an interconnected micro-pixel design was adopted. In addition, it was found that an LED design with interconnected micro-pixels separated by the n-AlGaN contact metal was very efficient in achieving the desired uniform current pumping for DUV-C LEDs, and devices with emission at 255 nm with 1-mW DC and 3.4-mW pulse power and corresponding maximum quantum efficiencies measured were 0.14% (under dc) and 0.3% (under pulse pumping). **Figure 7** shows images obtained from a charge-coupled device (CCD) camera with conventional geometry and micro-pixel-designed UV LEDs during CW operation. Changes in color indicate nonuniform emission due to spatial variations in current injection.

6.01.4.1.2 Effective thermal management of LEDs

One of the major drawbacks of employing sapphire as the substrate is that the DUV LEDs fabricated on it suffer from excessive self-heating under CW operation. This is caused by a combination of factors, such as poor thermal conductivity of sapphire, higher operating voltages resulting in eddy current losses, and low emission

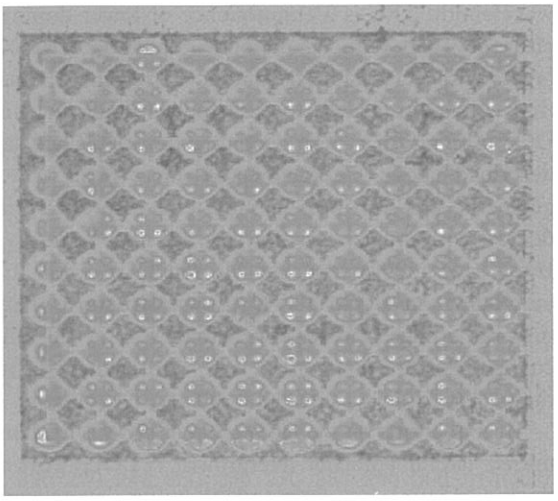

Figure 7 A charge-coupled-device (CCD) image of a micro-pixel ultraviolet light-emitting device (UV LED; total active of the junction is 220 μm^2) under continuous-wave bias condition showing the reduction of lateral current crowding and thereby reducing Joule heating.

efficiencies. Under typical CW operation, most of the sapphire-based DUV LEDs suffer from excessive self-heating due to the relatively higher operating voltages (which result in eddy current losses), low emission efficiencies, and poor thermal conductivity of the sapphire (0.35 W cm^{-1} K^{-1}). In an attempt to mitigate the device self-heating problem, Chitnis *et al.* (2002, 2003) employed flip-chip packaging. In this method, the diced LED chip is mounted in a flip-chip configuration on a high thermal conductivity 175 W mK^{-1} insulating AlN carrier with thermo-compression gold bonding. The AlN carrier with flip-chip UV LED is then mounted on a gold-coated header (**Figure 8(a)**). **Figure 8(b)** presents the DC optical power as a function of pump current for the standard and the flip-chip packaged LEDs. As can be seen from the graph, the performance of the device is improved by the flip-chip packaging technique. The saturation current (which is indicative of device self-heating) increased for flip-chip package, thereby enabling higher output power with higher input drive currents. Moreover, the slope of the curve improved due to better light extraction after flip-chip packaging.

Several groups have also started research efforts aimed at developing DUV LEDs with vertical conduction (Kawasaki *et al.*, 2006; Zhou *et al.*, 2006). For the reported works, the DUV LEDs are grown over sapphire substrates with a GaN buffer layer. This buffer layer allows the lift-off of the sapphire substrates and a backside n-contact, resulting in a vertical conduction

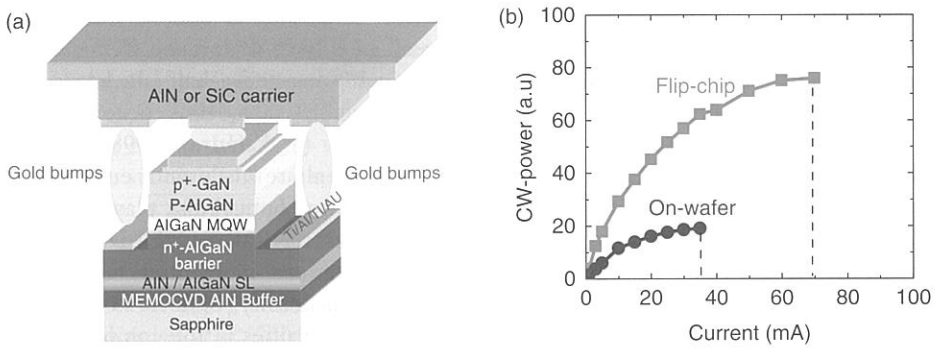

Figure 8 (a) Schematic of a flip-chip packaged deep ultraviolet light-emitting device (UV LED). (b) DC output power of standard and flip-chip mounted UV LEDs vs. pump current. (a) From Asif Khan M (2008) Vertical conduction strategy cranks up UV LED output power. *Compound Semiconductors Magazine* April 1.

geometry. However, the use of GaN buffer layer degrades the overall quality of the LED epilayers, leading to performance levels well below those for lateral geometry devices. The first successful fabrication of a large-area vertical-conduction 280-nm DUV LED over sapphire with AlN buffer layers has been fabricated by Adivarahan *et al.* (2009). For this vertical geometry DUV LED, laser lift-off was used to remove the sapphire substrate and form a backside n-contact to achieve vertical conduction (**Figures 9(a)** and **9(b)**). Similar to their visible counterparts, the vertical-geometry devices provide an excellent vehicle to produce large-area DUV LED lamps. They are expected to have much higher output powers due to the ability of sustaining much higher pump currents (as high as 1 A) and a substantial increase in the light extraction efficiency. It is reported that at a CW pump current of 200 mA, a high output power of 5.2 mW is achieved. This is the highest value of stable CW power reported for a single-chip 280-nm emission DUV LED.

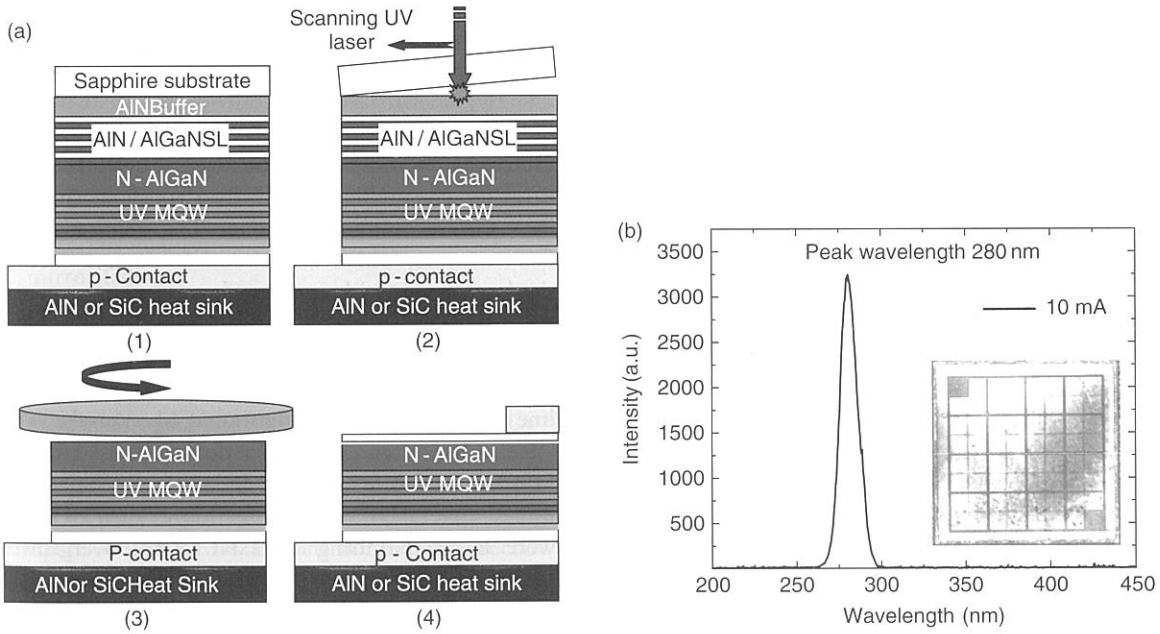

Figure 9 (a) Schematic of the formation process of vertically conducting deep ultraviolet light-emitting device (UV LED) by removing sapphire substrate by laser-assisted lift-off. (b) Electroluminescence spectrum of a vertical-conducting 280-nm LED (inset) n-AlGaN surface of the LED structure after the removal of sapphire by laser lift-off and AlN and superlattice layers by lapping and polishing. (a) From Asif Khan M (2008) Vertical conduction strategy cranks up UV LED output power. *Compound Semiconductors Magazine* April 1.

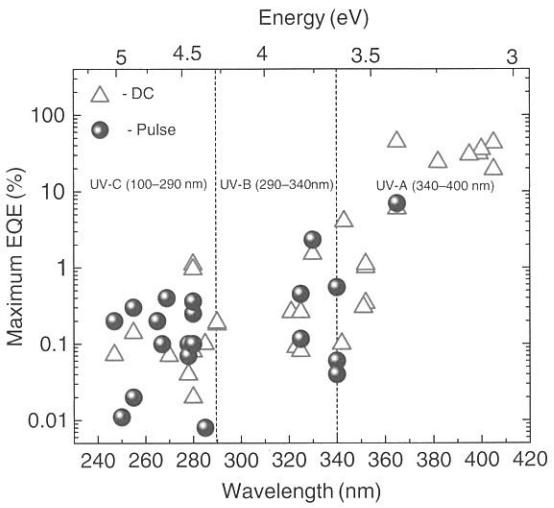

Figure 10 Summarized plot of maximum external quantum efficiency reported for continuous-wave (CW) (open) and pulse (closed) operations of ultraviolet light-emitting devices (UV LEDs).

Despite the material and device challenges associated with growth of very-wide-band-gap III-nitride AlInGaN materials, UV LEDs have advanced from less than 0.1% EQE to 1–10%, depending on emission wavelength, over the past 10 years. While the production of these devices is expected to ramp up, there are great challenges lying ahead. As seen from **Figure 10**, the efficiency of DUV LEDs is still not comparable to that of UV-A devices. An increase of the EQE up to ~10% must be achieved via further device optimization. The reduction of defects and improvements in doping in AlGaN layers with high Al molar fraction are of great importance for improving the efficiency of DUV-C emitters. Native single-crystal AlN substrates as well as innovative doping solutions must be considered. Another challenge is the light extraction, where novel encapsulation materials transparent down to ~200 nm should be explored.

6.01.5 UV Laser Diodes

In the early 1990s when the III-nitride-based blue LEDs were commercialized, researchers realized that blue and violet LDs were well within the reach. The lack of compact solid-state light sources in blue–violet UV region of the spectrum stimulated the development of growth techniques and prompted research on fabrication procedures for nitride-based materials. LDs occupy a specific and important place in this area, and violet (405 nm)-emitting nitride-based LDs have undergone tremendous progress in the past one-and-a-half decades with lifetimes exceeding 10 000 h, thus becoming commercially acceptable (Nakamura, 1998). Currently, most nitride lasers are made with emission at 405 nm for use in Blu-ray optical disk players (Hecht, 2008).

New shorter-wavelength LDs might find immediate applications in frontier technologies, such as super high-density optical storage systems, since recording densities in the compact disk are proportional to approximately the reciprocal of the wavelength squared. Other important applications include high-resolution laser printers, chemical sensing equipment, projection full-color displays, position location systems, bioagent detection and control, biotechnology applications, fine photolithography, and many more. The semiconductor laser has a number of unique advantages when compared against other coherent light sources: high efficiency, robustness, high speed, higher reliability, and potentially lower cost. A semiconductor UV LD would be a welcome replacement for the notoriously unreliable He–Cd gas laser. However, design and manufacturing of LDs itself is a much more complex problem in comparison with LEDs and requires even higher quality of materials to achieve the needed electrical and optical confinements in combination with low optical loss and high optical gain. Additional challenges present themselves in the device design, namely, the tiny laser cavities require low-loss waveguides with cladding layers featuring abrupt interfaces for optical confinement, as well as structures for channeling the electron and hole currents into the recombination zone. The realization of facet mirrors, which are smooth enough to define the laser cavity with very low losses, needs a special approach as well.

The first nitride-based injection laser, a device utilizing an InGaN active layer yielding an emission line at 405 nm, was demonstrated by Akasaki *et al.* (1995). Nakamura *et al.* also demonstrated nitride-based LDs later in 1996. In 1997, RT-operating 2-mW violet LDs, with lifetime longer than 10 000 h, were fabricated using epitaxial lateral overgrowth (ELOG)-grown GaN. Basically, over the next few years, rapid and impressive improvements in the performance of those nitride-based lasers were achieved predominantly by Nakamura and his co-workers at Nichia Chemical Industries. Those early efforts on nitride-based LDs usually covered the blue-to-near-UV (380–450 nm) spectral range.

Following these developments, LDs, which operate in the near-UV down to 360 nm, have been demonstrated (Nagahama *et al.*, 2001a, 2001b, 2002; Kneissl *et al.*, 2003, 2003a, 2003b, 2003c; Saitoh *et al.*, 2003). There are now nitride LDs with various different improvements, such as LDs with distributed Bragg reflectors (Cho *et al.*, 2000; Marinelli *et al.*, 2001; Saitoh *et al.*, 2003; Wang *et al.*, 2002), high-power output (Asano *et al.*, 2002; Nagahama *et al.*, 2000; Skierbiszewski *et al.*, 2005), and even different microcavity design (Kneissl *et al.*, 2004; Asano *et al.*, 2002). LDs reported by different groups have usually operated at RT under both pulsed and CW current-injection regimes and the designs are typically based on combinations of the InGaN/GaN/AlGaN heterostructure system. The lasing threshold has been as low as a few kA cm^{-2}, whereas output powers can typically reach up to several tens of milliwatts, although there are several cases where even hundreds of milliwatts have been emitted. All these LDs were based on optical transitions below the GaN bandgap and the active regions always included at least a small percentage of In. The aluminum content in alloys of AlInGaN or AlGaN was extremely low.

The attention was later focused on the results on LDs, where the light emission range has been expanded beyond the GaN band gap, that is, with the wavelength shorter than $\sim$ 360 nm. As mentioned earlier in this chapter, the shift of the wavelength toward deeper UV regions has been a challenging task basically due to the problems related with the incorporation of higher amount of Al into the nitride alloys. In this regard, the main problems in LD fabrication are:

1. materials quality;
2. mirror facets;
3. optical confinement; and
4. operation lifetime.

AlGaN materials of high quality (crack-free, low TDDs) with relatively high concentrations of Al are necessary, since we need to confine sufficient carriers in the QW in order to invert the population. In order to do so, very high injection levels are required in comparison with LEDs, and any nonradiative recombination paths will cause serious heating of the material. Such nonradiative losses would result in an increase of the lasing threshold or even the vanishing of the population inversion. High-quality mirror facets are necessary in order to obtain reasonable feedback in the cavity. Cleaving of nitrides on substrates, which are a different material, especially sapphire, is challenging. The cladding layers should contain a sufficiently high content of Al in order to provide a significant decrease in refractive index and thus effectively confine the coherent light within the active layer. Again, this causes strain and often cracking of the layers. Finally, the reported lifetimes of the UV LDs are quite short, too short from the commercial viewpoint. Hence, no wonder that only a small number of research efforts have been undertaken on UV LDs, and, consequently, only a limited number of reports have been published so far (Edmond *et al.*, 2004; Iida *et al.*, 2004a, 2004b; Kneissl *et al.*, 2003a, 2003b; Masui *et al.*, 2003; Yoshida *et al.*, 2007, 2008a, 2008b). The reported wavelength region of laser emission spans only 336–360 nm. Obviously, there has not been an breakthrough in the UV-LD technology, since these optical transitions still are very close to the GaN band gap. The shift of the lasing line toward the UV region has basically been achieved either due to rather small Al incorporation into alloys or just because of sufficient quantum confinement in very narrow QWs.

The basic structure of these near-UV LDs is similar to the ones operating in longer-wavelength regions. **Figure 11** shows a typical schematic diagram of the LD structure along with the possible energy-band configuration. In all the cases, the MOCVD growth technique has been employed. Notably, sapphire was used as substrate (Masui *et al.*, 2003; Kneissl *et al.*, 2003a, 2003b; Iida *et al.*, 2004a, 2004b; Yoshida *et al.*, 2007, 2008a, 2008b), and only Edmond *et al.* (2004) have successively applied SiC substrates. However, in all the cases, special measures were undertaken in order to reduce dislocation and other defect densities in the layers. Two very effective approaches for greatly reducing the defects, such as TDs, are the use of ELOG (Nam *et al.*, 1997) and facet-controlled epitaxial overgrowth (FACELO) (Iida *et al.*, 2004b; Yoshida *et al.*, 2008a, 2008b)". With the ELOG approach, a thin film of GaN is deposited over a sapphire substrate, and this film is then coated with an insulator such as SiO_2. Stripes are then etched in the oxide back to the GaN, and then a second nitride growth sequence is undertaken, where the new nitride material only grows up through the stripes. The new GaN film also grows laterally over the SiO_2 surface, and this lateral material can be nearly free of defects, allowing the fabrication of excellent laser structures over it (Mukai *et al.*, 1998). In the process of fabricating such devices, a few authors successively applied LT deposition for buffer layer or additional interlayer for

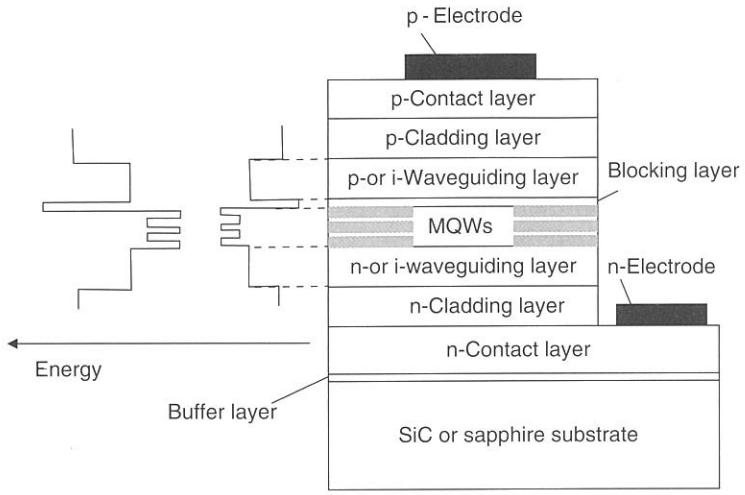

Figure 11 Typical schematic of the ultraviolet light-emitting device (UV LD) and possible energy-band diagram.

suppressing crack generation before attempting to deposit the actual LD structure (Kneissl *et al.*, 2003b; Iida*et al.*, 2004a, 2004b).

Most often, the active LD region consisted of several QWs (Edmond *et al.*, 2004; Iida *et al.*, 2004a, 2004b; Kneissl *et al.*, 2003a, 2003b) or even a single QW (Masui *et al.*, 2003) formed either with GaN (Iida *et al.*, 2004a, 2004b; Yoshida *et al.*, 2007), AlInGaN (Masui *et al.*, 2003; Kneissl *et al.*, 2003a; Edmond, 2004), or AlGaN (Kneissl *et al.*, 2003b; Yoshida *et al.*, 2008a, 2008b), serving as the well material. Typical widths of LD ridges are from 2 to 20 μm, whereas cavity lengths vary from 400 to 1500 μm. As an example, a specific LD structure, reported by Iida and co-workers (Iida *et al.*, 2004b), is analyzed. The active region of the LD was aligned on the ELOG region to provide material with low TDD. The n-contact layer consisted of a 4-μm-thick $Al_{0.18}Ga_{0.82}N$ layer, as well as an additional n-cladding layer. Then, an unintentionally doped $Al_{0.08}Ga_{0.92}N$ waveguiding layer (120 nm), three pairs of GaN (3 nm)/$Al_{0.08}Ga_{0.92}N$ (8 nm) MQW to form the active layer, an unintentionally doped $Al_{0.08}Ga_{0.92}N$ waveguiding layer (120 nm), a p-type $Al_{0.25}Ga_{0.75}N$ (20 nm) electron-blocking layer, a p- $Al_{0.18}Ga_{0.82}N$ (700 nm) cladding layer, and p^+-GaN (20 nm) contact layer were successively stacked. The laser cavity mirrors were formed by cleaving. Similar LD structures have also been successfully applied by other authors. The dopants of Si and Mg are typically used for n- and p-doping, respectively. In 2008, Yoshida *et al.* reported an AlGaN-based UV LD with an emission wavelength of 342.3 by current injection. In this case, a low-dislocation-density AlGaN layer with an AlN mole fraction of 0.3 was grown on sapphire substrate using a hetero-FACELO method to fabricate the laser. An AlGaN MQW structure was then grown on the high-quality AlGaN layer. When excited with 10-ns pulses at a 5-kHz repetition rate, 342.3-nm lasing was observed. The threshold current density reported for this laser is 8.7 kA cm^{-2}. The peak output power is 16 mW and the estimated differential EQE (DEQE) is 8.2%. Subsequently, the same authors (Yoshida *et al.*, 2008b) demonstrated a LD with the lowest emission wavelength (336 nm) reported so far. The device operated under RT pulsed current mode. The laser structure included a 2.8-μm-thick Si-doped $Al_{0.3}Ga_{0.7}N$ contacting layer, a 600-nm $Al_{0.3}Ga_{0.7}N$ cladding layer, a 90-nm-thick $Al_{0.16}Ga_{0.84}N$, and a 20-nm-thick p-AlGaN layer. MQW structure comprised the layers of $Al_{0.06}Ga_{0.94}N$ (well) and $Al_{0.16}Ga_{0.84}N$ (barrier).

Spectral properties of the LD obtained by Masui *et al.* (2003), namely, electroluminescence spectra at current densities below threshold (**Figure 12(a)**) and above threshold (**Figures 12(b)** and **12(c)**) are presented in **Figure 12**. **Figure 13** shows typical voltage versus current characteristics and light output versus current characteristics of the LD under pulsed condition, which operated at the wavelength of 350.9 nm (Iida *et al.*, 2004).

The precursor of future practical device designs for injection lasers operating in deeper regions of the UV spectrum must be as a first step of the realization of efficient photoluminescence and even stimulated emission in this range using optical pumping.

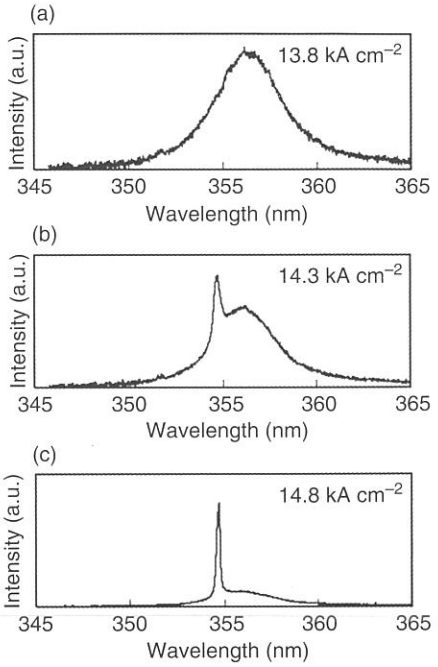

Figure 12 Emission spectra of ultraviolet light-emitting devices (UV LDs), composed of $Al_{0.09}Ga_{0.91}N$ waveguiding layers and $Al_{0.14}Ga_{0.86}N/Al_{0.09}Ga_{0.91}N$ cladding layers at different current densities. From Masui N, Matsuyama Y, Yanamoto T, Kozaki T, Nagahama S, and Mukai T (2003) 365 nm ultraviolet laser diodes composed of quaternary AlInGaN alloy. *Japanese Journal of Applied Physics* 42: L1318–L1320.

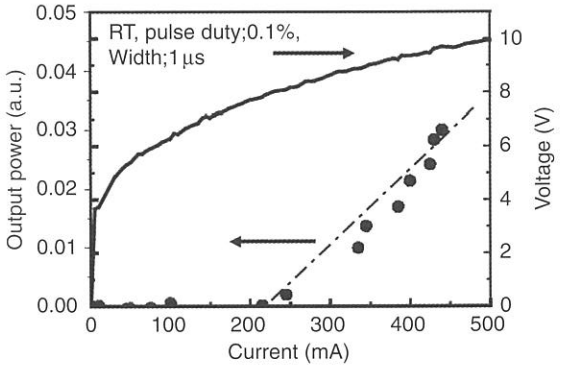

Figure 13 Voltage vs. current characteristic and light output vs. current characteristic of ultraviolet-laser diode (UV-LD) under pulsed condition at room temperature. Iida K, Kawashima T, Miyazaki A, *et al.* (2004) Laser diode of 350.9 nm wavelength grown on sapphire substrate by MOVPE. *Journal of Crystal Growth* 272: 270–273.

Currently, there are some new materials and improved structures with better quality, and a number of recent results seem to be promising in this regard. There are several reports on lasing in this

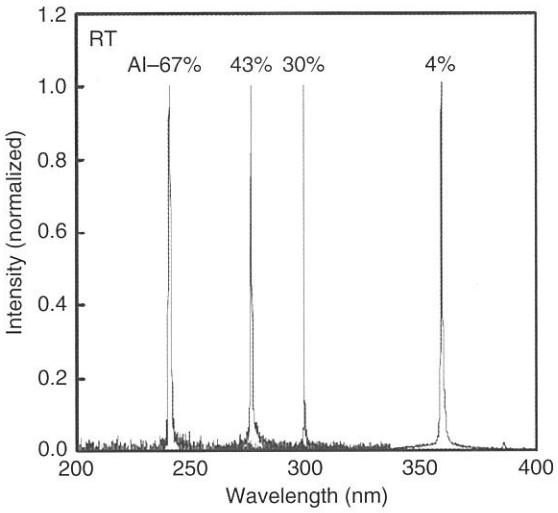

Figure 14 Lasing spectra of 354.5-nm AlGaN multiple quantum-well (MQW) laser under optical pumping. Reproduced from Takano T, Ohtaki Y, Narita Y, and Kawanishi H (2004) Improvement of crystal quality of AlGaN multi quantum well structure by combination of flow-rate modulation epitaxy and AlN/GaN multi-buffer layer and resultant lasing at deep ultra-violet region. *Japanese Journal of Applied Physics* 43: L1258–L1260, with permission from Japan Society of Applied Physics.

deeper UV region under photoexcitation in nitride-based MQWs. A stimulated emission line at 258 nm was observed in $Al_{0.5}Ga_{0.5}N/AlN$ MQWs grown on a bulk single-crystalline AlN template under strong selective photoexcitation of the QWs. Improvement of crystal quality of AlGaN MQW structure by combination of flow-rate modulation epitaxy and a new AlN/GaN multi-buffer layer allowed the authors to achieve lasing at 241 nm at RT. Even shorter-wavelength lasing (231.8 nm) was reported in AlGaN MQWs grown on a SiC substrate under photoexcitation at 20 K. **Figure 14** illustrates typical lasing spectra of a preliminary AlGaN MQW laser under optical pumping with different Al concentrations in the QW and the quantum barrier obtained by Takano *et al.* More recently, Shatalov *et al.* (2006) reported the first ever RT stimulated emission at 214 nm under pulsed condition using high-quality AlN layers that were grown over patterned sapphire substrates by a PLOG process. **Figure 15** shows the stimulated edge-emission spectra from the PLOG AlN film for the $E \parallel c$ and the $E \perp c$ polarizations. As seen from **Figure 14**, the stimulated emission signal was strongly polarized with $E \parallel c$ (transverse magnetic (TM) mode).

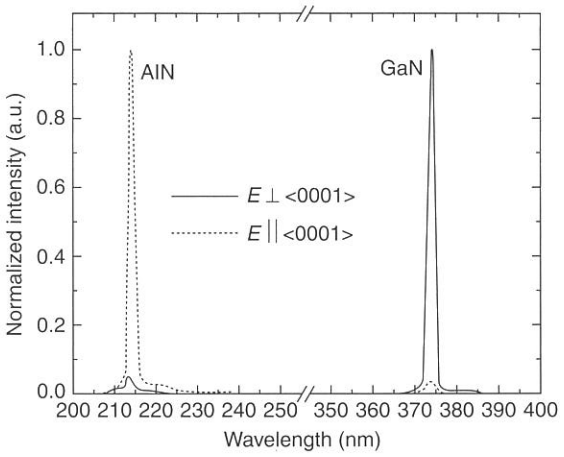

Figure 15 Stimulated edge-emission spectra of AlN (214 nm) and GaN for transverse electric (TE) and transverse magnetic (TM) polarizations. Reproduced from Shatalov M, Gaevski M, Adivarahan V, and Khan A (2006) Room-temperature stimulated emission from AlN at 214 nm. *Japanese Journal of Applied Physics* 45: L1286–L1288, with permission from Japan Society of Applied Physics.

These observations are in agreement with previous reports that suggest the stimulated emission from $Al_xGa_{1-x}N$ ($x \geq 0{:}65$) and AlN to be strongly polarized with $E \| c$ due to the dominance of the TM optical gain (Chow and Kneissl, 2005; Kawanishi *et al.*, 2006a, 2006b). This is in contrast to GaN, where the stimulated edge-emission signal is transverse electric (TE) polarized ($E \perp c$) due to the dominance of TE optical gain as well as the higher facet reflectivity (lower threshold) for the TE mode. For comparison, we also measured the edge stimulated emission spectrum for a GaN layer grown by MOCVD on sapphire. These data, presented in **Figure 14**, confirm the expected polarization differences. Similar difference in polarization properties was also found for $Al_xGa_{1-x}N$ multiple QW structures with different Al content.

LEDs have been stretched deep into UV region (down to 210 nm) because their operating conditions are much less demanding when compared with the LDs. On the other hand, electrically driven diode lasers remain stuck in the near-UV region and the shortest reported wavelength has decreased by just about 1 nm in the last 5 years. However, there are some very promising new approaches and we are entitled to expect in the near future a further shift of the nitride-based UV LD emission toward shorter wavelengths. A fully functional DUV nitride-based injection laser lies just over the horizon, especially because of the increasing availability of bulk nitride substrates and improvement in growth techniques.

6.01.6 Summary

Driven by the need for efficient, compact, and robust solid-state UV optical sources, massive research efforts have been undertaken in the past two decades to develop III-nitride-based UV and DUV emitters. Despite several fundamental problems, such as control of heteroepitaxy and doping, high efficiency near UV LEDs, extremely short wavelength UV LED, and CW operation of UV LD have been achieved and several of them have been already commercialized. There are still many great challenges left to be solved and need research focus. Development of alternative precursors for MOCVD growth of AlGaN may improve control of heteroepitaxy and minimize impurity incorporation. Improvements in growth techniques and the availability of nitrides bulk substrates should trigger massive improvement of device performance in the near future. Problem of p-type doping of AlGaN with high Al concentration will likely be the major obstacle for achieving DUV LEDs with efficiencies as high as 5–10%. Large difference in Al molar fraction between waveguide and clad layers required for efficient waveguiding in UV LD structures also poses a significant challenge in the growth and strain control of these AlGaN-based layers. Alternative concepts for LED and LD device design, involving approaches of nano-electronics and nano-photonics, should be considered and these may overcome some of the above-mentioned fundamental problems.

References

Adivarahan V, Heidari A, Zhang B, *et al.* (2009) Vertical injection thin film deep ultraviolet light emitting diodes with AlGaN multiple-quantum wells active region. *Applied Physics Express* 2: 092102.

Adivarahan V, Sun WH, Chitnis A, *et al.* (2004a) 250 nm AlGaN light-emitting diodes. *Applied Physics Letters* 85: 2175–2177.

Adivarahan V, Wu S, Chitnis A, *et al.* (2002) AlGaN single-quantum-well light-emitting diodes with emission at 285 nm. *Applied Physics Letters* 81: 3666–3668.

Adivarahan V, Wu S, Sun WH, *et al.* (2004b) High-power deep ultraviolet light-emitting diodes based on a micro-pixel design. *Applied Physics Letters* 85: 1838–1840.

Adivarahan V, Wu S, Zhang JP, *et al.* (2004c) High-efficiency 269 nm emission deep ultraviolet light-emitting diodes. *Applied Physics Letters* 84: 4762–4764.

Akasaki I, Amano H, Sota S, Sakai S, Tanaka T, and Koike M (1995) Stimulated emission by current injection from an AlGaN/GaN/GaInN quantum well device. *Japanese Journal of Applied Physics* 34: L1517–L1519.

Allerman AA, Crawford MH, Fischer AJ, *et al.* (2004) Growth and design of deep-UV (240–290 nm) light emitting diodes using AlGaN alloys. *Journal of Crystal Growth* 272: 227–241.

Amano H, Sawaki N, Akaskai I, and Toyoda Y (1986) Metalorganic vapor phase epitaxial growth of a high quality GaN film using an AlN buffer layer. *Applied Physics Letters* 48: 353–355.

Amano H, Sawaki N, Akasaki I, and Toyoda Y (1989) P-type conduction in Mg-doped GaN treated with low-energy electron beam irradiation (LEEBI). *Japanese Journal of Applied Physics* 28: L2112–L2114.

Asano T, Takeya M, Tojyo T, *et al.* (2002) High-power 400-nm-band AlGaInN-based laser diodes with low aspect ratio. *Applied Physics Letters* 80: 3497–3499.

Balakrishnan K, Bandoh A, Iwaya M, Kamiyama S, Amano H, and Akasaki I (2007) Influence of high temperature in the growth of low dislocation content AlN bridge layers on patterned 6H-SiC substrates by metalorganic vapor phase epitaxy. *Japanese Journal of Applied Physics* 46: L307–L310.

Bernardini F, Fiorentini V, and Vanderbilt D (1997) Spontaneous polarization and piezoelectric constants of III–V nitrides. *Physical Review* B 56: R10024–R10027.

Bilenko Y, Lunev A, Hu X, *et al.* (2005) 10 Milliwatt pulse operation of 265 nm AlGaN light emitting diodes. *Japanese Journal of Applied Physics* 44: L98–L100.

Bockowski M, Grzegory I, Krukowski S, *et al.* (2004) Deposition of bulk GaN from solution in gallium under high N_2 pressure on silicon carbide and sapphire substrates. *Journal of Crystal Growth* 270: 409–419.

Boroditsky M, Krauss TF, Coccioli R, Vrijen R, Bhat R, and Yablonovitch E (1999) Light extraction from optically pumped light-emitting diode by thin-slab photonic crystals. *Applied Physics Letters* 75: 1036–1038.

Bykhovsky AD, Gelmont BL, and Shur MS (1997) Elastic strain relaxation and piezoeffect in GaN–AlN, GaN–AlGaN and GaN–InGaN superlattices. *Journal of Applied Physics* 81: 6332.

Chen Z, Qhalid Fareed RS, Gaevsk M, *et al.* (2006) Pulsed lateral epitaxial overgrowth of aluminum nitride on sapphire substrates. *Applied Physics Letters* 89: 081905–081907.

Chitnis A, Adivarahan V, Shatalov M, *et al.* (2002a) Submilliwatt operation of AlInGaN based multifinger-design 315 nm light emitting diode (LED) over sapphire substrate. *Japanese Journal of Applied Physics* 41: L320–L322.

Chitnis A, Adivarahan V, Zhang JP, *et al.* (2003a) Milliwatt power AlGaN quantum well deep ultraviolet light emitting diodes. *Physica Status Solidi (a)* 200: 99–101.

Chitnis A, Pachipulusu R, Mandavilli V, *et al.* (2002b) Low-temperature operation of AlGaN single-quantum-well light-emitting diodes with deep ultraviolet emission at 285 nm. *Applied Physics Letters* 81: 2938–2940.

Chitnis A, Sun J, Mandavilli V, *et al.* (2002c) Self-heating effects at high pump currents in deep ultraviolet light-emitting diodes at 324 nm. *Applied Physics Letters* 81: 3491–3493.

Chitnis A, Zhang JP, Adivarahan V, *et al.* (2002d) 324 nm Light emitting diodes with milliwatt powers. *Japanese Journal of Applied Physics* 41: L450–L451.

Chitnis A, Zhang JP, Adivarahan V, *et al.* (2003b) Improved performance of 325-nm emission AlGaN ultraviolet light-emitting diodes. *Applied Physics Letters* 82: 2565–2567.

Cho J, Cho S, Kim BJ, *et al.* (2000) InGaN/GaN multi-quantum well distributed Bragg reflector laser diode. *Applied Physics Letters* 76: 1489–1491.

Chow WW and Kneissl M (2005) Laser gain properties of AlGaN quantum wells. *Journal of Applied Physics* 98: 114502.

Deng J, Bilenko Y, Lunev A, *et al.* (2007) 247 nm ultra-violet light emitting diodes. *Japanese Journal of Applied Physics* 46: L263–L264.

Edmond J, Abare A, Bergman M, *et al.* (2004) High efficiency GaN-based LEDs and lasers on SiC. *Journal of Crystal Growth* 272: 242–250.

Fareed Q, Adivarahan V, Gaevski M, *et al.* (2007) Metal-organic hydride vapor phase epitaxy of $Al_xGa_{1-x}N$ films over sapphire. *Japanese Journal of Applied Physics* 46: L752–L754.

Fischer AJ, Allerman AA, Crawford MH, *et al.* (2004) Room-temperature direct current operation of 290 nm light-emitting diodes with milli-watt power levels. *Applied Physics Letters* 84: 3394–3396.

Gao H and Nix WD (1999) Surface roughening of heteroepitaxial thin films. *Annual Review of Materials Science* 29: 173–209.

Gaska R, Chen C, Yang J, *et al.* (2002) Deep-ultraviolet emission of AlGaN/AlN quantum wells on bulk AlN. *Applied Physics Letters* 81: 4658–4660.

Goepfert ID, Schubert EF, Osinsky A, Norris PE, and Faleev NN (2000) Experimental and theoretical study of acceptor activation and transport properties in p-type $Al_xGa_{1-x}N$/GaN superlattices. *Journal of Applied Physics* 88: 2030–2038.

Guo X and Schubert EF (2001) Current crowding and optical saturation effects in GaInN/GaN light-emitting diodes grown on insulating substrates. *Applied Physics Letters* 89: 081121.

Han J, Crawford MH, Shul RJ, *et al.* (1998) AlGaN/GaN quantum well ultraviolet light emitting diodes. *Applied Physics Letters* 73: 1688–1690.

Han J, Figiel JJ, Petersen GA, Myers SM, Crawford MH, and Banas MA (2000) Metal-organic vapor-phase epitaxial growth and characterization of quaternary AlGaInN. *Japanese Journal of Applied Physics* 39: 2372–2375.

Han J, Waldrip KE, Lee SR, *et al.* (2001) Control and elimination of cracking of AlGaN using low-temperature AlGaN interlayers. *Applied Physics Letters* 78: 67–69.

Hanlon A, Pattison PM, Kaeding JF, Sharma R, Fini P, and Nakamura S (2003) 292 nm AlGaN single-quantum well light emitting diodes grown on transparent AlN base. *Japanese Journal of Applied Physics* 42: L628–L630.

Hecht J (2008) Semiconductor UV lasers: Materials are a tough challenge for ultraviolet diode lasers. *Laser Focus World* 45(12). http://www.laserfocusworld.com/display_article/346708/12/none/none/Feat/PHOTONIC-FRONTIERS:-SEMICONDUCTOR-UV-LASERS:-Materials-are-a-tough-challenge-for-ultraviolet-diode-laser (accessed February 2010).

Hirayama H, Kinoshita A, Hirata A, and Aoyagi Y (2001) Growth and optical properties of quaternary InAlGaN for 300 nm band UV-emitting devices. *Physica Status Solidi (a)* 188: 83–89.

Hirayama H, Kinoshita A, Yamabi T, *et al.* (2002) Marked enhancement of 320–360 nm ultraviolet emission in quaternary $In_xAlyGa_{1-x-y}N$ with In-segregation effect. *Applied Physics Letters* 80: 207–209.

Hu X, Deng J, Pala N, *et al.* (2003) AlGaN/GaN heterostructure field-effect transistors on single-crystal bulk AlN. *Applied Physics Letters* 82: 1299–1301.

Hwang J, Schaff WJ, Eastman LF, Bradley ST, Brillson LJ, and Look DC (2002) Si doping of high-Al-mole fraction $Al_xGa_{1-x}N$ alloys with rf plasma-induced molecular-beam-epitaxy. *Applied Physics Letters* 81: 5192–5194.

Iida K, Kawashima T, Miyazaki A, *et al.* (2004a) Laser diode of 350.9 nm wavelength grown on sapphire substrate by MOVPE. *Journal of Crystal Growth* 272: 270–273.

Iida K, Kawashima T, Miyazaki A, *et al.* (2004b) 350.9 nm UV laser diode grown on low-dislocation-density AlGaN. *Japanese Journal of Applied Physics* 43: L499–L500.

Imura M, Nakano K, Fujimoto N, *et al.* (2006a) High-temperature metal-organic vapor phase epitaxial growth of AlN on sapphire by multi transition growth mode method varying V/III ratio. *Japanese Journal of Applied Physics* 45: 8639–8643.

Imura M, Nakano K, Kitano T, *et al.* (2006b) Microstructure of epitaxial lateral overgrown AlN on trench-patterned AlN template by high- temperature metal-organic vapor phase epitaxy. *Applied Physics Letters* 89: 221901–221902.

Imura M, Nakano K, Fujimoto N, *et al.* (2007) Dislocations in AlN epilayers grown on sapphire substrate by high-temperature metal-organic vapor phase epitaxy. *Japanese Journal of Applied Physics* 46: 1458–1462.

Jeon SR, Gherasimova M, Ren Z, *et al.* (2004) High performance AlGaInN ultraviolet light-emitting diode at the 340 nm wavelength. *Japanese Journal of Applied Physics* 43: L1409–L1412.

Jeys TH, Desmarais L, Lynch EJ, and Ochoa JR (2003) Development of a UV-LED-based biosensor. In: Carapezza EM (ed.) *Proceedings of SPIE, Volume 5071, Sensors, and Command, Control, Communications, and Intelligence (C3I) Technologies for Homeland Defense and Law Enforcement II,* vol. 5071, pp. 234–240. Orlando, FL: SPIE.

Jin SX, Li J, Li JZ, Lin JY, and Jiang HX (2000) GaN microdisk light emitting diodes. *Applied Physics Letters* 76: 631–633.

Kamiyama S, Iwaya M, Hayashi N, *et al.* (2001) Low-temperature-deposited AlGaN interlayer for improvement of AlGaN/GaN heterostructure. *Journal of Crystal Growth* 223: 83–91.

Kamiyama S, Iwaya M, Amano H, and Akasaki I (2002) Heteroepitaxial technology for high-efficiency UV light-emitting diode. *Opto-Electronics Review* 10: 225–229.

Kato N, Sato S, Sumii T, *et al.* (2007) High-speed growth of AlGaN having high-crystalline quality and smooth surface by high-temperature MOVPE. *Journal of Crystal Growth* 298: 215–218.

Kawaguchi Y, Sugahara G, Mochida A, Shimamoto T, Ishibashi A, and Yokogawa T (2003) Low-dislocation density AlGaN layer by air-bridged lateral epitaxial growth. *Physica Status Solidi (c)* 0: 2107–2110.

Kawanishi H, Senuma M, and Nukui T (2006a) Anisotropic polarization characteristics of lasing and spontaneous surface and edge emissions from deep-ultraviolet ($\lambda \approx 240$ nm) AlGaN multiple-quantum-well lasers. *Applied Physics Letters* 89: 041126.

Kawanishi H, Senuma M, Yamamoto M, Niikura E, and Nukui T (2006b) Extremely weak surface emission from (0001) c-plane AlGaN multiple quantum well structure in deep-ultraviolet spectral region. *Applied Physics Letters* 89: 081121.

Kawasaki K, Koike C, Aoyagi Y, and Takeuchi M (2006) Vertical AlGaN deep ultraviolet light emitting diode emitting at 322 nm fabricated by the laser lift-off technique. *Applied Physics Letters* 89: 261114.

Khan MA, Adivarahan V, Zhang JP, *et al.* (2001) Stripe geometry ultraviolet light emitting diodes at 305 nanometers using quaternary AlInGaN multiple quantum wells. *Japanese Journal of Applied Physics* 40: L1308–L1310.

Khan MA (2006) AlGaN multiple quantum well based deep UV LEDs and their applications. *Physica Status Solidi (a)* 203: 1764–1770.

Khan MA, Balakrishnan K, and Katona T (2008) III-nitride based ultraviolet light-emitting diodes. *Nature Photonics* 2: 77–81.

Khan MA, Kuzina JN, Olson DT, George T, and Pike WT (1993) GaN/AlN digital alloy short-period superlattices by switched atomic layer metalorganic chemical vapor deposition. *Applied Physics Letters* 63: 3470–3472.

Khan MA, Kuznia JN, Skogman RA, Olson DT, Mac Millan M, and Choyke WJ (1992a) Low pressure metal-organic chemical vapor deposition of AlN over sapphire substrates. *Applied Physics Letters* 61: 2539–2541.

Khan MA, Shatalov M, Maruska HP, Wang HM, and Kuokstis E (2005) III-nitride UV devices. *Japanese Journal of Applied Physics* 44: 7191–7206.

Khan MA, Skogman RA, Van Hove JM, Krishnankutty S, and Kolbas RM (1990) Photoluminescence characteristics of AlGaN–GaN–AlGaN quantum well) Photoluminescence characteristics of AlGaN–GaN–AlGaN quantum wells. *Applied Physics Letters* 56: 1257–1259.

Khan MA, Skogman RA, Van Hove JM, Olson DT, and Kuznia JN (1992b) Atomic layer epitaxy of GaN over sapphire using switched metal-organic chemical vapor deposition. *Applied Physics Letters* 60: 1366–1368.

Khan MA, Wu S, Sun WH, *et al.* (2004) 255 nm interconnected micro-pixel deep ultraviolet light emitting diodes. In: *Proceedings of IEEE International Electron Devices Meeting.* San Francisco, CA, USA 13–15 December.

Khan MA, Yang JW, Simin G, Gaska R, Shur MS, and Loye HCZ (2000) Lattice and energy band engineering in AlInGaN/GaN heterostructures. *Applied Physics Letters* 76: 1161–1163.

Khizar M, Fan FY, Kim KH, Lin JY, and Jiang HX (2005) Nitride deep-ultraviolet light-emitting diodes with microlens array. *Applied Physics Letters* 86: 173504–173506.

Kim KH, Li J, Jin SX, Lin JY, and Jiang HX (2002) III-nitride ultraviolet light-emitting diodes with delta doping. *Applied Physics Letters* 83: 566–568.

Kim KH, Fan ZY, Khizar M, Nakarmi ML, Lin JY, and Jiang HX (2004) AlGaN-based ultraviolet light-emitting diodes grown on AlN epilayers. *Applied Physics Letters* 85: 4777–4779.

Kim ST, Lee YJ, Moon DC, Hong CH, and Yoo TK (1998) Preparation and properties of free-standing HVPE grown GaN substrates. *Journal of Crystal Growth* 194: 37–42.

Kinoshita A, Hirayama H, Ainoya M, Aoyagi Y, and Hirata A (2000) Room-temperature operation at 333 nm of $Al_{0.03}Ga_{0.97}N$/$Al_{0.25}Ga_{0.75}$ quantum-well light-emitting diodes with Mg-doped superlattice layers. *Applied Physics Letters* 77: 175–177.

Kipshidze G, Kuryatkov V, Borisov B, Holtz M, Nikishin S, and Temkin H (2001) AlGaInN-based ultraviolet light-emitting diodes grown on Si(111). *Japanese Journal of Applied Physics Letters* 80: 3682–3684.

Kipshidze G, Kuryatkov V, Zhu K, *et al.* (2003) AlN/AlGaInN superlattice light-emitting diodes at 280 nm. *Journal of Applied Physics* 93: 1363.

Kneissl M, David WT, Teepe M, Miyashita N, and Johnson NM (2003a) Continuous-wave operation of ultraviolet InGaN/InAlGaN multiple-quantum-well laser diodes. *Applied Physics Letters* 82: 2386–2388.

Kneissl M, David WT, Teepe M, Miyashita N, and Johnson NM (2003b) Ultraviolet AlGaN multiple-quantum-well laser diodes. *Applied Physics Letters* 82: 4441–4443.

Kneissl M, David WT, Teepe M, Miyashita N, and Johnson NM (2003c) Ultraviolet InAlGaN multiple-quantum-well laser diodes. *Physica Status Solidi (a)* 200: 118–121.

Kneissl M, David WT, Teepe M, *et al.* (2004) Current-injection spiral-shaped microcavity disk laser diodes with unidirectional emission. *Applied Physics Letters* 84: 2485–2487.

Kozodoy P, Hansen M, Den Baars SP, and Mishra UK (1999) Enhanced Mg doping efficiency in $Al_{0.2}Ga_{0.8}N$/GaN superlattices. *Applied Physics Letters* 74: 3681–3683.

Kozodoy P, Smorchkova YP, Hansen M, *et al.* (1999) Polarization-enhanced Mg doping of AlGaN/GaN superlattices. *Applied Physics Letters* 75: 2444–2446.

Kuryatkov V, Zhu K, Borisov Chandolu BA, *et al.* (2003) Electrical properties of p–n junctions based on superlattices of AlN/AlGa(In)N. *Applied Physics Letters* 83: 1319–1321.

Lefebvre P, Gil B, Allegre J, *et al.* (1999) Quantum-confined Stark effect and recombination dynamics of spatially indirect excitons in MBE-grown GaN–AlGaN quantum wells. *MRS Internet Journal of Nitride Semiconductor Research* 4S1: G3.69.

Mair RA, Zeng KC, Lin JY, *et al.* (1997) Optical properties of GaN/AlGaN multiple quantum well microdisks. *Applied Physics Letters* 71: 2898–2900.

Malikova L, Huang YS, Pollak FH, Feng ZC, Schurman M, and Stall RA (1997) Temperature dependence of the energies and broadening parameters of the excitonic interband transitions in $Ga_{0.95}Al_{0.05}N$. *Solid State Communications* 103: 273–278.

Marinelli C, Bordovsky M, Sargent LJ, *et al.* (2001) Design and performance analysis of deep-etch air/nitride distributed Bragg reflector gratings for AlInGaN laser diodes. *Applied Physics Letters* 79: 4076–4080.

Masui N, Matsuyama Y, Yanamoto T, Kozaki T, Nagahama S, and Mukai T (2003) 365 nm ultraviolet laser diodes composed of quaternary AlInGaN alloy. *Japanese Journal of Applied Physics* 42: L1318–L1320.

Mayes K, Yasan A, McClintock R, *et al.* (2004) High-power 280 nm AlGaN light-emitting diodes based on an asymmetric single-quantum well. *Applied Physics Letters* 84: 1046–1048.

McIntosh FG, Boutros KS, Roberts JC, Bedair SM, Piner EL, and El-Mastry NA (1996) Growth and characterization of AlInGaN quaternary alloys. *Applied Physics Letters* 68: 40–42.

Mickevicius J, Aleksiejnas R, Shur MS, *et al.* (2005) Lifetime of nonequilibrium carriers in high-Al-content AlGaN epilayers. *Physica Status Solidi (a)* 202: 126–130.

Micronews (2009) UV LEDs challenge the traditional $500M UV lamp business. http://www.i-micronews.com/reports/UV-LED-Market-2009/80 (accessed November 2009).

Morita D, Sano M, Yanamoto M, Murayama T, Nagahama S, and Mukai T (2002) High output power 365 nm ultraviolet light emitting diode of GaN-free structure. *Japanese Journal of Applied Physics* 41: L1434–L1436.

Motoki K, Okahisa T, Matsumot N, *et al.* (2001) Preparation of large freestanding GaN substrates by hydride vapor phase epitaxy using GaAs as a starting substrate. *Japanese Journal of Applied Physics* 40: L140–L143.

Mukai T, Takekawa K, and Nakamura S (1998) InGaN-based blue light-emitting diodes grown on epitaxially laterally overgrown GaN substrates. *Japanese Journal of Applied Physics* 37: L839–L841.

Nagahama S, Iwasa N, Senoh M, *et al.* (2000) High-power and long-lifetime InGaN multi-quantum-well laser diodes grown on low-dislocation-density GaN substrates. *Japanese Journal of Applied Physics* 39: L647–L650.

Nagahama S, Yanamoto T, Sano M, and Mukai T (2001a) Ultraviolet GaN single quantum well laser diodes. *Japanese Journal of Applied Physics* 40: L785–L787.

Nagahama S, Yanamoto T, Sano M, and Mukai T (2001b) Characteristics of ultraviolet laser diodes composed of quaternary $Al_xIn_yGa_{(1-x-y)}N$. *Japanese Journal of Applied Physics Letters* 80: 3682–3684.

Nagahama S, Yanamoto T, Sano M, and Mukai T (2002) Study of GaN-based laser diodes in near ultraviolet region. *Japanese Journal of Applied Physics* 41: 5–10.

Nakamura S (1991) GaN growth using GaN buffer layer. *Japanese Journal of Applied Physics* 30: L1705–L1707.

Nakamura S (1998) InGaN/GaN/AlGaN-based laser diodes with an estimated lifetime of longer than 10,000 hours. *Materials Research Society Symposia Proceedings* 482: 1145–1150.

Nakamura S, Mukai T, Senoh M, and Iwasa N (1992) Thermal annealing effects on p-type Mg-doped GaN films. *Japanese Journal of Applied Physics* 31: L139–L142.

Nakarmi ML, Kim KH, Li J, Lin JY, and Jiang HX (2003) Enhanced p-type conduction in GaN and AlGaN by Mg-δ-doping. *Applied Physics Letters* 82: 3041–3043.

Nam OK, Bremser MD, Zheleva TS, and Davis RF (1997) Lateral epitaxy of low defect density GaN layers via organometallic vapor phase epitaxy. *Applied Physics Letters* 71: 2638–2640.

Nikishin SA, Kuryatkov VV, Chandolu A, *et al.* (2003) Deep ultraviolet light emitting diodes based on short period superlattices of AlN/AlGa(In)N. *Japanese Journal of Applied Physics* 42: L1362–L1364.

Nishida T and Kobayashi N (1999) 346 nm emission from AlGaN multi-quantum-well light emitting diode. *Physica Status Solidi (a)* 176: 45–48.

Nishida T, Makimoto T, Saito H, and Ban T (2004) AlGaN-based ultraviolet light-emitting diodes grown on bulk AlN substrates. *Applied Physics Letters* 84: 1002–1004.

Nishida T, Saito H, and Kobayashi N (2001) Efficient and high-power AlGaN-based ultraviolet light-emitting diode grown on bulk GaN. *Applied Physics Letters* 79: 711–713.

Nishida T, Saito H, Kumakura K, Makimoto T, and Kobayashi N (2000) Selectively enhanced Mg incorporation into AlGaN barrier layer of strained layer superlattice. In: *Proceedings of International Workshop on Nitride Semiconductors (IWN2000)*, IPAP Conference Series 1, p. 725–727. Tokyo: IPAP.

Oder TN, Kim KH, Lin JY, and Jiang HX (2004) III-nitride blue and ultraviolet photonic crystal light emitting diodes. *Applied Physics Letters* 84: 466–468.

Oder TN, Shakya J, Lin JY, and Jiang HX (2003) III-nitride photonic crystals. *Applied Physics Letters* 83: 1231–1233.

Okada N, Fujimoto N, Kitano T, *et al.* (2006) Thermodynamic aspects of growth of AlGaN by high-temperature metal organic vapor phase epitaxy. *Japanese Journal of Applied Physics* 45: 2502–2504.

Okada N, Kato N, Sato S, *et al.* (2007) Epitaxial lateral overgrowth of a-AlN layer on patterned a-AlN template by HT-MOVPE. *Journal of Crystal Growth* 300: 141–144.

Otsuka N, Tsujimura A, Hasegawa Y, Sugahara G, Kume M, and Ban Y (2000) Room temperature 339 nm emission from $Al_{0.13}Ga_{0.87}N/Al_{0.10}Ga_{0.90}N$ double heterostructure light-emitting diode on sapphire substrate. *Japanese Journal of Applied Physics* 39: L445–L448.

Peng H, Makarona E, He Y, *et al.* (2004) Ultraviolet light-emitting diodes operating in the 340 nm wavelength range and application to time-resolved fluorescence spectroscopy. *Applied Physics Letters* 85: 1436–1438.

Rojo JC, Slack GA, Morgan K, Raghothamachar B, Dudley M, and Schowalter LJ (2001) Report on the growth of bulk aluminum nitride and subsequent substrate preparation. *Journal of Crystal Growth* 231: 317–321.

Rojo JC, Slack GA, Morgan K, Raghothamachar B, Dudley M, and Schowalter LJ (2002) Growth and characterization of epitaxial layers on aluminum nitride substrates prepared from bulk, single crystals. *Journal of Crystal Growth* 240: 508–512.

Saitoh T, Kumagai M, Wang H, *et al.* (2003) Highly reflective distributed Bragg reflectors using a deeply etched semiconductor/air grating for InGaN/GaN laser diodes. *Applied Physics Letters* 82: 4426–4428.

Saxler A, Mitchel WC, Kung P, and Razeghi M (1999) Aluminum gallium nitride short-period superlattices doped with magnesium. *Applied Physics Letters* 74: 2023–2025.

Shan W, Ager JW, III, Yu KM, *et al.* (1999) Dependence of the fundamental band gap of $Al_xGa_{1-x}N$ on alloy composition and pressure. *Applied Physics Letters* 85: 8505.

Shatalov M, Chitnis A, Mandavilli V, *et al.* (2003) Time-resolved electroluminescence of AlGaN-based light-emitting diodes with emission at 285 nm. *Applied Physics Letters* 82: 167–169.

Shatalov M, Gaevski M, Adivarahan V, and Khan MA (2006) Room-temperature stimulated emission from AlN at 214 nm. *Japanese Journal of Applied Physics* 45: L1286–L1288.

Shatalov M, Simin G, Adivarahan V, *et al.* (2002a) Lateral current crowding in deep UV light emitting diodes over sapphire substrate. *Japanese Journal of Applied Physics* 41: 5083–5087.

Shatalov M, Simin G, Zhang JP, *et al.* (2002b) Gan/AlGan p-channel inverted heterostructure JFET. *IEEE Electron Device Letters* 23: 452–454.
Shur MS, Bykhovski AD, Gaska R, Yang JW, Simin G, and Khan MA (2000) Accumulation hole layer in p-GaN/AlGaN heterostructures. *Applied Physics Letters* 76: 3061–3063.
Silveira E, Freitas JA, Jr., Kneissl M, *et al.* (2004) Near-band edge cathodoluminescence of an AlN homoepitaxial film. *Applied Physics Letters* 84: 3501.
Skierbiszewski C, Wasilewski ZR, Siekacz M, *et al.* (2005) Blue–violet InGaN laser diodes grown on bulk GaN substrates by plasma-assisted molecular-beam epitaxy. *Applied Physics Letters* 86: 011114.
Smeeton TM, Humphreys CJ, Barnard JS, and Kappers MJ (2006) The impact of electron beam damage on the detection of indium-rich localization centres in InGaN quantum wells using transmission electron microscopy. *Journal of Materials Science* 41: 2729–2737.
Strategies Unlimited's Report – PennWell Corporation (2009) GaN substrates: Performance comparisons and market assessment – 2009. *Report SC-29.* http://downloads.pennnet.com/pnet/research/66/gan2009_substrate comparo-toc.pdf (accessed November 2009).
Sun W, Zhang JP, Chen CQ, Fareed Q, Yang JW, and Asif Khan M (2004) Continuous wave milliwatt power AlGaN light emitting diodes at 280 nm. Japanese. *Journal of Applied Physics* 43: L1419–L1421.
Sun WH, Zhang JP, Adivarahan V, *et al.* (2004) AlGaN-based 280 nm light-emitting diodes with continuous wave powers in excess of 1.5 mW. *Applied Physics Letters* 85: 531–533.
Taniyasu S, Kasu M, and Makimoto T (2006) An aluminium nitride light-emitting diode with a wavelength of 210 nanometres. *Nature* 441: 325–328.
Waltereit P, Brandt O, Trampert A, *et al.* (2000) Nitride semiconductors free of electrostatic fields for efficient white light-emitting diodes. *Nature* 406: 865–868.
Wang H, Kumagai M, Tawara T, *et al.* (2002) Fabrication of an InGaN multiple-quantum-well laser diode featuring high reflectivity semiconductor/air distributed Bragg reflector. *Applied Physics Letters* 81: 4703.
Wang HM, Zhang JP, Chen CQ, Fareed Q, Yang JW, and Asif Khan M (2002) AlN/AlGaN superlattices as dislocation filter for low-threading-dislocation thick AlGaN layers on sapphire. *Applied Physics Letters* 81: 604–606.
Wang T, Liu YH, Lee YB, Ao JP, Bai J, and Sakai S (2002) 1 mW AlInGaN-based ultraviolet light-emitting diode with an emission wavelength of 348 nm grown on sapphire substrate. *Applied Physics Letters* 81: 2508–2510.
Wu S, Adivarahan V, Shatalov M, Chitnis A, Sun WH, and Asif Khan M (2004) Micro-pixel design milliwatt power 254 nm emission light emitting diodes. *Japanese Journal of Applied Physics* 43: L1035–L1037.
Yasan A, Mc Clintock R, Mayes K, Darvish SR, Kung P, and Razeghi M (2002) Top-emission ultraviolet light-emitting diodes with peak emission at 280 nm. *Applied Physics Letters* 81: 801–803.
Yasan A, Mc Clintock R, Mayes K, *et al.* (2003) 4.5 mW operation of AlGaN-based 267 nm deep-ultraviolet light-emitting diodes. *Applied Physics Letters* 83: 4701–4703.
Yoshida H, Yamashia Y, Kuwabara M, and Kan H (2008a) A 342-nm ultraviolet AlGaN multiple-quantum-well laser diode. *Nature Photonics* 2: 551–554.
Yoshida H, Yamashita Y, Kuwabara M, and Kan H (2008b) Demonstration of an ultraviolet 336 nm AlGaN multiple-quantum-well laser diode. *Applied Physics Letters* 93: 241106.
Yoshida H, Yasufumi T, Kuwabara M, Amano H, and Kan H (2007) Entirely crack-free ultraviolet GaN/AlGaN laser diodes grown on 2-inch sapphire substrate. *Japanese Journal of Applied Physics* 46: 5782–5784.
Zhang JP, Adivarahan V, Wang HM, *et al.* (2001a) Quaternary AlInGaN multiple quantum wells for ultraviolet light emitting diodes. *Japanese Journal of Applied Physics* 40: L921–L924.
Zhang JP, Asif Khan M, Sun WH, *et al.* (2002a) Pulsed atomic-layer epitaxy of ultrahigh-quality $Al_xGa_{1-x}N$ structures for deep ultraviolet emissions below 230 nm. *Applied Physics Letters* 81: 4392–4394.
Zhang JP, Chitnis A, Adivarahan V, *et al.* (2002b) Milliwatt power deep ultraviolet light-emitting diodes over sapphire with emission at 278 nm. *Applied Physics Letters* 81: 4910–4912.
Zhang JP, Hu X, Bilenko Y, *et al.* (2004) AlGaN-based 280 nm light-emitting diodes with continuous-wave power exceeding 1 mW at 25 mA. *Applied Physics Letters* 85: 5532–5534.
Zhang JP, Kuokstis E, Fareed Q, *et al.* (2001b) Pulsed atomic layer epitaxy of quaternary AlInGaN layers. *Applied Physics Letters* 79: 925–927.
Zhang JP, Wang HM, Gaevski ME, *et al.* (2002c) Crack-free thick AlGaN grown on sapphire using AlN/AlGaN superlattices for strain management. *Applied Physics Letters* 80: 3542–3544.
Zhang JP, Wang HM, Sun WH, *et al.* (2003a) High-quality AlGaN layers over pulsed atomic-layer epitaxially grown AlN templates for deep ultraviolet light-emitting diodes. *Journal of Electronic Materials* 32: 364–370.
Zhang JP, Wu S, Rai S, *et al.* (2003b) AlGaN multiple-quantum-well-based, deep ultraviolet light-emitting diodes with significantly reduced long-wave emission. *Applied Physics Letters* 83: 3456–3458.
Zhang W and Meyer BK (2003) Growth of GaN quasi-substrates by hydride vapor phase epitaxy. *Physica Status Solidi (c)* 0: 1571–1582.
Zhou L, Epler JE, Krames MR, *et al.* (2006) Vertical injection thin-film AlGaN/AlGaN multiple-quantum-well deep ultraviolet light-emitting diodes. *Applied Physics Letters* 89: 241113.
Zhu TG, Denyszyn JC, Chowdhury U, and Wong MM (2002) AlGaN–GaN UV light-emitting diodes grown on SiC by metal-organic chemical vapor deposition. *IEEE Journal of Selected Topics in Quantum Electronics* 8: 298–301.
Zhu TG, Chowdhury U, Denyszyn JC, Wong MM, and Dupuis RD (2003) AlGaN/AlGaN UV light-emitting diodes grown on sapphire by metalorganic chemical vapor deposition. *Journal of Crystal Growth* 248: 548–551.

Further Reading

Adivarahan V, Chitnis A, Zhang JP, *et al.* (2001) Ultraviolet light-emitting diodes at 340 nm using quaternary AlInGaN multiple quantum wells. *Applied Physics Letters* 79: 4240–4242.
Adivarahan V, Zhang JP, Chitnis A, *et al.* (2002) Sub-milliwatt power III-N light emitting diodes at 285 nm. *Japanese Journal of Applied Physics* 41: L435–L436.
Akasaka T, Nishia T, Makimoto T, and Kobayashi N (2004) An InGaN-based horizontal-cavity-surface-emitting laser diode. *Applied Physics Letters* 84: 4104–4106.
Khan MA, Shatalov M, Maruska HP, Wang HM, and Kuokstis E (2007) III-nitride UV devices. *Japanese Journal of Applied Physics* 44: 7191–7206.
Guo X and Schubert EF (2001) Current crowding and optical saturation effects in GaInN/GaN light-emitting diodes grown on insulating substrates. *Applied Physics Letters* 78: 3337–3339.

He Y, Song YK, Nurmikko AV, *et al.* (2004) Optically pumped ultraviolet AlGaInN quantum well laser at 340 nm wavelength. *Applied Physics Letters* 84: 463–465.

Jeon CW, Gu E, and Dawson MD (2005) Mask-free photolithographic exposure using a matrix-addressable micropixellated AlInGaN ultraviolet light-emitting diode. *Applied Physics Letters* 86: 221105.

Mukai T, Morita D, Yanamoto M, *et al.* (2005) Investigation of optical-output-power degradation in 365-nm UV-LEDs. *Physica Status Solidi (c)* 3: 2211–2214.

Nakamura S, Senoh M, Nagahama S, *et al.* (1996) InGaN-based multi-quantum-well-structure laser diodes. *Japanese Journal of Applied Physics* 35: L74–L76.

Nakamura S, Senoh M, Nagahama S, *et al.* (1996) InGaN multi-quantum-well-structure laser diodes with cleaved mirror cavity facets. *Japanese Journal of Applied Physics* 35: L217–L220.

Nakamura S, Senoh M, Nagahama S, *et al.* (2006) InGaN multi-quantum-well structure laser diodes grown on $MgAl_2O_4$ substrates. *Applied Physics Letters* 68: 2105–2107.

Ohba Y and Hatano A (1996) Growth of high-quality AlN and AlN/GaN/AlN heterostructure on sapphire substrate. *Japanese Journal of Applied Physics* 35: L1013–L1015.

Ohba Y, Sato R, and Kaneko K (2001) Two-dimensional growth of AlN and GaN on lattice-relaxed $Al_{0.4}Ga_{0.6}N$ buffer layers prepared with high-temperature-grown AlN buffer on sapphire substrates and fabrication of multiple-quantum-well structures. *Japanese Journal of Applied Physics* 40: L1293–L1296.

Shatalov M, Chitnis A, Adivarahan V, *et al.* (2001) Band-edge luminescence in quaternary AlInGaN light-emitting diodes. *Applied Physics Letters* 78: 817–819.

Shatalov M, Zhang J, Chitnis AS, Yang J, Simin G, and Asif Khan M (2002) Deep ultraviolet light-emitting diodes using quaternary AlInGaN multiple quantum wells. *IEEE Journal of Selected Topics in Quantum Electronics* 8: 302–309.

Takano T, Narita Y, Horiuchi A, and Kawanishi H (2004) Room-temperature deep-ultraviolet lasing at 241.5 nm of AlGaN multiple-quantum-well laser. *Applied Physics Letters* 84: 3567–3569.

Takano T, Ohtaki Y, Narita Y, and Kawanishi H (2004) Improvement of crystal quality of AlGaN multi quantum well structure by combination of flow-rate modulation epitaxy and AlN/GaN multi-buffer layer and resultant lasing at deep ultra-violet region. *Japanese Journal of Applied Physics* 43: L1258–L1260.

Yilmaz I, Gaska R, Fareed Q, *et al.* (2003) Stimulated emission at 258 nm in AlN/AlGaN quantum wells grown on bulk AlN substrates. *Materials Research Society Proceedings* 764: C69.